



# Cerebellar dysfunction in the *mdx* mouse model of Duchenne muscular dystrophy: An electrophysiological and behavioural study

Cynthia Prigogine<sup>1,2</sup> | Javier Marquez Ruiz<sup>3</sup> | Ana Maria Cebolla<sup>1</sup>  |  
Nicolas Deconinck<sup>4</sup> | Laurent Servais<sup>5</sup> | Philippe Gailly<sup>6</sup> | Bernard Dan<sup>1,7</sup> |  
Guy Cheron<sup>1,2</sup> 

<sup>1</sup>Laboratory of Neurophysiology and Movement Biomechanics, Université Libre de Bruxelles, Brussels, Belgium

<sup>2</sup>Laboratory of Electrophysiology, Université de Mons, Mons, Belgium

<sup>3</sup>Division of Neurosciences, Universidad Pablo de Olavide, Sevilla, Spain

<sup>4</sup>Department of Pediatric Neurology, Hôpital Universitaire des Enfants Reine Fabiola, Brussels, Belgium

<sup>5</sup>Institut de Myologie, APHP Pitié-Salpêtrière, Paris, France

<sup>6</sup>Laboratory of Cell Physiology, Université Catholique de Louvain, Brussels, Belgium

<sup>7</sup>Rehabilitation Hospital Inkendaal, Vlezenbeek, Belgium

## Correspondence

Guy Cheron, Laboratory of Neurophysiology and Movement Biomechanics, Université Libre de Bruxelles, Brussels, Belgium.  
Email: [guy.cheron@ulb.be](mailto:guy.cheron@ulb.be)

## Funding information

Fonds de Recherche de l'Université de Mons, Belgium; Fonds de recherche de l'Université Libre de Bruxelles, Belgium; Leibniz Fond, Belgium; Brain & Society Foundation (Belgium); Fonds National de la Recherche Scientifique (FNRS), Belgium; Université Libre de Bruxelles and Université de Mons, Belgium; Brain and Society Foundation; Leibniz Fond; the Fonds National de la Recherche Scientifique (FNRS), Belgium

Edited by: Maxime Assous

## Abstract

Patients with Duchenne muscular dystrophy (DMD) commonly show specific cognitive deficits in addition to a severe muscle impairment caused by the absence of dystrophin expression in skeletal muscle. These cognitive deficits have been related to the absence of dystrophin in specific regions of the central nervous system, notably cerebellar Purkinje cells (PCs). Dystrophin has recently been involved in GABA<sub>A</sub> receptors clustering at postsynaptic densities, and its absence, by disrupting this clustering, leads to decreased inhibitory input to PC. We performed an *in vivo* electrophysiological study of the dystrophin-deficient muscular dystrophy X-linked (*mdx*) mouse model of DMD to compare PC firing and local field potential (LFP) in alert *mdx* and control C57Bl/10 mice. We found that the absence of dystrophin is associated with altered PC firing and the emergence of fast (~160–200 Hz) LFP oscillations in the cerebellar cortex of alert *mdx* mice. These abnormalities were not related to the disrupted expression of calcium-binding proteins in cerebellar PC. We also demonstrate that cerebellar long-term depression is altered in alert *mdx* mice. Finally, *mdx* mice displayed a force weakness, mild impairment of motor coordination and balance during behavioural tests. These findings demonstrate the existence of cerebellar dysfunction in *mdx* mice. A

**List of abbreviations:** CSs, complex spikes; DMD, Duchenne muscular dystrophy; LFP, local field potential; LTD, long-term depression; *mdx*, muscular dystrophy X-linked mouse; PC, Purkinje cell; SRTT, serial reaction time task; SSs, simple spikes.

similar cerebellar dysfunction may contribute to the cognitive deficits observed in patients with DMD.

#### KEYWORDS

cerebellum, cognitive impairment, Duchenne muscular dystrophy, dystrophin, fast oscillations, long-term depression, *mdx*, Purkinje cells

## 1 | INTRODUCTION

Duchenne muscular dystrophy (DMD) is one of the most common congenital neuromuscular disorders in childhood, with a birth prevalence between 21.7 and 28.2 per 100,000 live male births (Orso et al., 2023). It is caused by mutations within the dystrophin gene, resulting in the absence or the disruption of dystrophin production (Amoasii et al., 2017). The absence of this cytoskeletal protein localized at the inner part of the muscle fibre membrane affects membrane stability and calcium homeostasis (Deconinck & Dan, 2007), resulting in muscle degeneration. Although several drugs arisen from recent clinical studies have been recently approved (Markati et al., 2022), the clinical evolution is severe, characterized by rapidly progressive muscle weakness and wasting leading to premature death due to cardiorespiratory complications. In addition to muscle impairment (Wallace & McNally, 2009), many patients show specific cognitive deficits that include learning, behavioural, emotional and memory impairment (Pascual-Morena, Caverro-Redondo, Álvarez-Bueno, et al., 2023). Full-scale IQ scores follow a normal distribution that is shifted 1 standard deviation below the population mean, with a higher prevalence of intellectual disability (Cotton et al., 2001), deficits in verbal working memory (Anderson et al., 1988; Dorman et al., 1988; Hinton et al., 2000; Leibowitz & Dubowitz, 1981) and impairments in praxis and executive function (Donders & Taneja, 2009; Hinton et al., 2000; Maresh et al., 2023; Mento et al., 2011; Wicksell et al., 2004). General academic achievement is also lower among boys with DMD compared to their unaffected siblings (Hinton et al., 2001, 2007).

The cognitive deficits in DMD have been hypothesized to relate to the loss of dystrophin in specific regions of the central nervous system (CNS) (Dubowitz & Crome, 1969; Uchino, Teramoto, Naoe, Yoshioka, et al., 1994; Kim et al., 1995). Dystrophin is exclusively localized at the postsynaptic densities of specific neuronal subtypes, namely pyramidal neurons of the cerebral neocortex, hippocampus (Lidov et al., 1990) and amygdala (Sekiguchi et al., 2009) and in cerebellar Purkinje cell (PC) where it is the most abundant (Knuesel et al., 1999;

Lidov et al., 1990). The cognitive profile in DMD includes specific impairments of implicit learning during the performance of a serial reaction time task (SRTT) (Vicari et al., 2018) that have been similarly observed in adults with diffuse or focal lesions in the cerebellum (Gómez-Beldarrain et al., 1998). Following the timing processing performed by the cerebellum (Avanzino et al., 2016), ischemic damage to the left cerebellum may induce a selective deficit in the SRTT realized with the left hand (Torriero et al., 2007). It has also been suggested that lack of P-type dystrophin in PC may account for impaired verbal working memory (Cyrułnik & Hinton, 2008) due to disruption of information rehearsal in the cerebrocerebellar loops that project from the lateral cerebellum (Cyrułnik & Hinton, 2008) to the ipsilateral dorsolateral prefrontal cortex (DLPFC) (Torriero et al., 2007).

Additional evidence supporting the role of dystrophin in cognition comes from studies of *mdx* (muscular dystrophy X-linked) mice, the full-length dystrophin-deficient murine model of DMD in which both brain and muscle full-length dystrophin isoforms are absent (Uchino, Teramoto, Naoe, Miike, et al., 1994). These mice display various cognitive and behavioural impairments, including deficits in passive avoidance (Muntoni et al., 1991), spatial learning (Vaillend et al., 2004) and memory deficits (Vaillend et al., 1995). In addition, Comim et al. (2019) reported the presence of neuroinflammation and depressive-anxiety-like behaviour in the *mdx* mice.

Dystrophin has been implicated in  $\gamma$ -aminobutyric acid (GABA<sub>A</sub>) receptor stabilization and clustering at postsynaptic densities of inhibitory synapses (Chamberlain et al., 1988; Knuesel et al., 1999; Nudel et al., 1988; Pereira da Silva et al., 2018; Zarrouki et al., 2022). Its loss causes dysfunctional signalling of these inhibitory synapses and leads to decreased inhibitory input. Interestingly, Sekiguchi et al. (2009) found that decreased inhibitory input to amygdala pyramidal neurons is related to enhanced fear and anxiety behaviours. Overall, the different forms of dystrophin play a role not only in cerebral development but also in several glutamatergic and GABAergic synaptic mechanisms. This could explain the increased incidence of epilepsy in DMD (Ramani et al., 2023) but also the partial rescue of central nervous phenotype in MDX following the post-natal

restoration of dystrophin (Hashimoto et al., 2022; Zarrouki et al., 2022).

Dystrophin presents several isoforms. Those that are expressed in the brain are Dp427, Dp140 and Dp71 mostly in the hippocampus, amygdala and temporal and frontal cortex (Doorenweerd et al., 2017). Dp427 is expressed in the cerebellum at the post-GABAergic synaptic side in PC (Fujimoto et al., 2023). The primary function of Dp140 is to anchor GABA<sub>A</sub> receptors to the postsynaptic membrane of GABAergic neurons (Knuesel et al., 1999). Dp140 also plays a role in the early central nervous system during the foetal stage and is implicated in dendrite development, transcription factor activity, neuron differentiation and chromatin modification (Naidoo & Anthony, 2020). Dp140 also plays an important role in glutamatergic transmission (Hashimoto et al., 2022). The role of Dp71 is less well understood and could also include the control of the glutaminergic pathway, as demonstrated in the climbing fibre-PC synapse (Helleringer et al., 2018). Electrophysiological studies have also demonstrated decreased inhibitory input to PC in *mdx* mice (Gorecki et al., 1991; Jung et al., 1991; Kueh et al., 2008; Lidov et al., 1990, 1993; Nudel et al., 1988).

Since cerebellar PC represents the sole integrative output of the cerebellar cortex, and their activity depends not only on intrinsic excitability but also on synaptic input, decreased inhibitory input due to GABA<sub>A</sub> clustering alteration may compromise their firing. Here, we tested this, by recording cerebellar electrophysiological activity and plasticity of PC in alert *mdx* mice, and assessed the related motor coordination, balance and motor learning which are functions traditionally attributed to the cerebellum.

We found that the absence of dystrophin was associated with altered PC activity, characterized by a significant increase in simple spike (SS) firing rate, regularity and rhythmicity. Moreover, the duration of the pause induced by complex spikes (CSs) in SS firing was significantly longer in *mdx* mice. We also found the emergence of fast (~160–200 Hz) local field potential (LFP) oscillation in the cerebellar cortex in alert *mdx* mice. While PC response to electrical stimulation of the whisker pad was similar in *mdx* and control mice, the cerebellar long-term depression (LTD) induced by an 8-Hz stimulation was disrupted in *mdx* mice. Finally, the behavioural results showed that while the rotarod test revealed no significant difference between *mdx* and control mice, the wire test, catwalk and runway demonstrated a force weakness, a mild impairment of motor coordination and balance but a conserved behavioural learning capacity in *mdx* mice. These findings confirm the existence of a cerebellar dysfunction in *mdx* mice that may contribute to cognitive

deficits seen in *mdx* mice and possibly in patients with DMD.

## 2 | MATERIALS AND METHODS

### 2.1 | Mice

In vivo electrophysiological recordings were performed on nine *mdx* (C57BL/10ScSn-Dmdmdx) and on eight wild-type (WT) control male mice (C57BL/10ScSn), age-matched (4–8 months), obtained from the Jackson Laboratory (Bar Harbor, Maine, USA). Behavioural studies were carried on 10 *mdx* and 11 WT male mice. Mice were kept in a standard room with a day/night rhythm of 06:00/18:00 at 21°C and 50%–60% humidity. All experiments were carried out during their light cycle. The experimental protocol was approved by the Ethical Committee of the University of Mons (UMons) and the Catholic University of Louvain (UCL) and conformed to European Union directive 609/86/EU and Belgian guidelines for the care and use of laboratory animals. Every effort was made to minimize the number of animals and their discomfort.

### 2.2 | In vivo electrophysiology in alert mice

#### 2.2.1 | Surgical preparation

Nine *mdx* and eight WT mice (aged 4–8 months) were surgically prepared 24 h before the first recording session (Cheron et al., 2004). Mice were anaesthetized with xylido-dihydrothiazin (10 mg/kg, i.p. Rompun<sup>®</sup>, Bayer) and ketamine (100 mg/kg, i.p. Ketalar<sup>®</sup>, Pzifer). Animals were administered an additional dose of xylido-dihydrothiazin (3 mg/kg) and ketamine (30 mg/kg) if they presented agitation or markedly increased breathing or heart rate during the procedure. In addition, local anaesthesia [0.5 mL of 20 mg/mL lidocaine and adrenaline (1:80,000, Xylocaine<sup>®</sup>, Astra Zeneca)] was administered subcutaneously during soft tissue removal. Two small bolts were cemented to the skull to immobilize the head during the recording session, and a silver reference electrode was placed on the surface of the parietal cortex. A craniotomy was performed at the level of the cerebellum by progressive bone abrasion using a dental drill. An acrylic recording chamber was constructed around the craniotomy and covered by a thin layer of bone wax (Ethicon<sup>®</sup>, Johnson & Johnson) in sterile conditions before and between recording sessions.

## 2.2.2 | In vivo electrophysiological recordings

Twenty-four hours after anaesthesia and surgical procedure, alert mice were restrained for the recording session. To minimize stress for the animals and movement artifacts, recordings were performed in a quiet room when the animals were calm in the setting. Criteria for PC recording and data analysis were the same as those used in previous studies (Cheron et al., 2004). Briefly, PC activity and cerebellar LFP were recorded in the vermis (lobules IV–VIII/IXa and IXb) and over Crus I and IIa using linearly arranged, quartz-insulated, platinum-tungsten fibre-microelectrodes (1.2–3 M $\Omega$  impedance, outer and shaft diameter of 80 and 25  $\mu$ m, respectively) with 250  $\mu$ m interelectrode spacing. Each microelectrode was mounted into a stretched elastic rubber tube enabling proper positioning via DC-micromotors (resolution of 0.27  $\mu$ m) (Eckhorn & Thomas, 1993).

## 2.2.3 | Data collection and analysis

The recorded signal was displayed continuously on an oscilloscope. After amplification (1000–2000 $\times$ ) and band-pass filtering (10 Hz to 10 kHz), LFP and unitary electrical activities were stored digitally at 20 kHz on a computer after conversion with an analogue-digital converter (Power 1401, CED $\text{\textcircled{c}}$ , Cambridge, UK). Off-line analyses were performed using the Spike 2 CED software (CED $\text{\textcircled{c}}$ , Cambridge, UK).

A neural signal was identified as a PC only if it presented two distinct types of spiking activity: SSs, characterized by a single depolarization (300–800  $\mu$ s) occurring at an average frequency of 50 Hz (20–200 Hz), and less frequent CSs (0.5–1.5 Hz), characterized by an initial fast depolarization (300–600  $\mu$ s) followed, in a relatively constant manner for the same PC, by smaller components of decreasing amplitude, called secondary spikes or spikelets, with a total duration of 8–25 ms. These two signals were considered as originating from the same PC when the CS produced a transient pause ( $\sim$ 15 ms) in SS firing. Discrimination between SS and CS was performed with Spike 2 CED software (waveform recognition) and controlled visually before analysis. The regularity of PC was measured using a coefficient of variation (CV) defined as the quotient between the standard deviation of the SS firing rate and the mean of the interspike intervals. Autocorrelation histograms were plotted for SS firing from a single PC (width = 1 s, bin size = 1 ms). The rhythmic frequency was defined as the reciprocal of the latency of the first peak in the autocorrelogram of SS firing (width = 1 s, bin size = 1.0 ms). Consequently,

rhythmic frequency could not be determined on flat autocorrelograms. The strength of the rhythmicity was quantified with a rhythm index (RI) introduced by Sugi-hara et al. (1995). Briefly, peaks and valleys were recognized if their heights and depths exceeded the mean baseline level  $\pm$  standard deviation (SD) (measured at time lags of 250–300 ms). RI was defined by the following formula:  $RI = a1/z + b1/z + a2/z + b2/z + \dots$ , in which  $a_i$  ( $i = 1, 2, \dots$ ) is the absolute value of the difference between the height of the  $i$ th peak and baseline level,  $b_i$  ( $i = 1, 2, \dots$ ) is the absolute value of the difference between the height of the  $i$ th valley and baseline level and  $z$  was the difference between the height of the zero time bin and the baseline level. In autocorrelograms with no significant peaks and valleys, a value of zero was given to the RI, and the activity was considered non-rhythmic.

Waveform averaging was performed with the corresponding function of Spike2 CED software on a 120-s minimum recording. CS duration was measured on the CS averaged trace during the analyzed recording and defined as the period between the first depolarization and the last secondary spike. The duration of SS pause was defined as the period between the beginning of the CS (first potential) and the beginning of the first SS after the CS. LFP was analyzed using a 4096-point fast Fourier transform (FFT) algorithm computed from a 15-s recording sample. FFT histogram results from 14 s of recording analyzed by a FFT size of 8096 with an Hanning window (resolution of 3.052 Hz) (4096 bins) and a filtering from 10 to 12,500 Hz.

## 2.2.4 | Cerebellar LFP plasticity

Using a paradigm previously described (Márquez-Ruiz & Cheron, 2012), we investigated the plasticity of cerebellar LFPs evoked by electrical stimulation of the whisker pad/region in six *mdx* mice and in six WT mice. An 8-Hz stimulation frequency was used to induce cerebellar LFP plasticity. LFP measurements elicited by single whisker pad electrical stimuli administered randomly every  $10 \pm 3$  s were performed 15 min before and 30 min after trains of electrical stimuli given at a frequency of 8 Hz for 10 min. Recordings were analyzed when a stable signal was present for longer than 60 s. Electrophysiological responses to electrical stimulation in the whisker region were assessed by the specific configuration of the LFP (which must show P1-N1-N2-P2-N3 components). As the P1/N1 component reflects the evoked activity in the mossy fibres of the granule cell layer, when this component was stable during the experiment, we assumed there was no extra cerebellar modification of the input

signals. The peak amplitudes and latencies of N2 and N3 components were used as indexes of the postsynaptic responses. These components were compared with the SS responses of the recruited PC. For amplitude and latency quantifications of N1, N2 and N3, 30 successive evoked field potentials were offline averaged to collect one average data point every 5 min. For peak-to-peak amplitude measurements, negative peaks were compared to the trough of the preceding positive wave. When the P1 positive peak was not evident, we used the inflection point observed in the averaged trace for the N1 measurement. For N3 measurements, the amplitude was set as the difference between the positive peak between N2 and N3 and the negative peak of N3. Latency was determined as the time difference between stimulus onset and N1, N2 or N3 averaged peaks. For comparisons between animals, amplitude values for each one of the LFP's components were normalized by the mean values obtained during the electrical stimuli randomly administered before the 8-Hz stimulation, for statistical analysis.

## 2.3 | Calcium-binding protein quantification in the cerebellum of mdx mice

### 2.3.1 | Immunofluorescence labelling

Mice were anaesthetized with ketamine (Ketalar 75 mg/kg) and xylazine (Rompun 5 mg/kg) solution. Mice were perfused transcardially with 4% paraformaldehyde in phosphate-buffered saline (PBS). The whole brain was removed. Samples were rinsed three times in cold PBS and cryoprotected in a sucrose gradient (10%, 20% then 30% sucrose/PBS) at 4°C. Tissues were embedded in PBS/15% sucrose/7.5% gelatin and frozen in isopentane at -25°C. Samples were cut (20 µm) in a sagittal plane using a Microm HM500 cryostat, and sections were collected on Superfrost Plus Slides (Thermoscientific, Pittsburgh, PA). Cryosections were dried at room temperature and stored at -20°C. For immunofluorescence, cryosections were saturated with PBS/10% horse serum/0.1% Triton for 30 min at room temperature. Slides were dip-rinsed with PBS. Primary antibodies diluted in PBS/10% horse serum/0.1% Tween were incubated overnight at 4°C. Slides were washed thrice in PBS/0.1% Tween and incubated with secondary antibodies and Hoescht 33342 (Sigma) in the same solution as for primary antibodies for 1 h at RT. After washing in PBS/0.1% Tween and PBS, slides were mounted with a fluorescent mounting medium (DAKO, Via Real, Carpinteria, CA, USA). Primary antibodies were rabbit anti-calbindin protein (1:10,000, Swant, CB38), goat anti-

Calretinin (1:5000), goat anti-parvalbumin (1:5000) and mouse anti-dystrophin (1:5, Novocastra, NCL-DYS1). Secondary antibodies from Life Technologies were diluted 1:2000. Pictures were taken with a Zeiss Axiovert 200 M inverted microscope (×20 fluorescence objective) (Zeiss Belgium, Zaventem, Belgium).

## 3 | MRNA ANALYSIS

Mice were sacrificed, and cerebella were dissected, snap-frozen in liquid nitrogen and stored at -80°C until processing. Total RNA was isolated from the cerebellum using TRIzol reagent (Ambion, Invitrogen) as described by the manufacturer. Recovery was 1 µg/mg of tissue. Reverse transcription and real-time quantitative polymerase chain reaction (PCR) were done as previously described (Zanou et al., 2012). Accession numbers for the sequences and primers used were parvalbumin, NM\_013645.3 (AGGATGAGCTGGGGTCCATT-TTTCAGCCACCAGAGTGGAG); calbindin, NM\_009788.4 (ATTCGACGCTGACGGAAGT-GTGGGTAAGACGTGAGCAA); calretinin, NM\_007586.1 (TGCCATGATGTC-CAAGAGCG-ATTCTCTTCGGTCCGGCAGGA); Slc1a6, NM\_009200.3 (GGTGGTGTGTTGCCCTTAT-CCAGGCAGCGAAAGTGATA); Gng13, NM\_022422.5 (CTGCTTTTGCTGTCTCTCCAA-CCAGTTGGTACTT-GAGGCTCT); and Cyclophilin D, BC019778 (CGTCCAGATGAGGAGTCGGA-TAAGCATGATCGGGAGGGTT) used as the reporter gene.

Primers were tested to avoid primer dimers, self-priming formation or nonspecific amplification. The primers were designed to have standardized optimal PCR conditions.

### 3.1 | Behavioural testing

Behavioural tests were done on 4-month-old mice (10 *mdx* vs 11 control male mice).

#### 3.1.1 | The accelerating rotarod

This test assesses the mouse ability to stay balanced on an accelerating (4 to 40 rpm over 300 s) rotating rod (Panlab-Bioseb, Vitrolle France). Mice received three trials per day for five consecutive days and were allowed to rest for at least 5 min between trials. The latency to fall off the Rotarod was recorded. Animals staying for 300 s were taken from the rotarod and recorded as 300 s. A retention test was performed 9 days after the last training session to assess long-term motor learning ability.

### 3.1.2 | The runway test

This test assesses the mouse's ability to go across an elevated narrow runway (100 cm long, 1.2 cm wide, 50 cm high) towards their home cage. Low obstacles, consisting of wood rods (1 cm diameter, 1.2 cm width), were placed every 10 cm to hinder their progression. Mice received five trials per day for four consecutive days. Crossing time, number of falls and number of times the feet slipped off the runway were noted. A retention test was performed 8 days after the last training session to assess long-term learning ability.

### 3.1.3 | The catwalk test

This test was used to assess the gait of spontaneously walking mice by a computer-assisted automated quantitative gait analysis system (Catwalk 7.1, Noldus; Wageningen, The Netherlands). Paw print recording allowed analysis of various aspects of walking steps such as the basis of support (Vandeputte et al., 2010). Three runs were performed per animal per day, for three consecutive days, and analysis was performed on the fastest uninterrupted run.

### 3.1.4 | The wire test

In this test, we have followed the protocol of Zanou et al. (2010). The mice were suspended by their forelimbs from a 1.5-mm-thick, 60-cm-long metallic wire at 45 cm above soft ground. The time until the mouse completely released its grasp and fell was recorded. Three trials were performed per session, with a 30-s recovery period between trials. The maximum time per trial was set to 180 s. For each mouse, the scores of the three trials were averaged.

## 3.2 | Statistical analysis

For in vivo electrophysiological and behavioural experiments, statistical differences between genotype groups were performed using the software R version 4.0.5. The normality of distributions was analyzed with Shapiro–Wilk tests; then, the homogeneity of variances ( $F$  tests) was analyzed. Depending on these analyses and normality of distribution of variables,  $T$  test or Wilcoxon Mann–Whitney tests were used appropriately. The outliers were also identified, and the effect of outliers removing was

checked. The results are reported as mean  $\pm$  SD and illustrated in box plots. The level of significance was set at  $p < 0.05$ . For the rotarod and runway, statistical differences between groups were compared using two-way repeated analysis of variance (ANOVA) with Bonferroni's post hoc test. For the catwalk test, statistical differences between groups were compared using Student's  $t$ -test with STATISTICA 6.0 statistical software package (StatSoft, Tulsa, Oklahoma, USA).

## 4 | RESULTS

### 4.1 | SS firing rate, regularity and rhythmicity are significantly increased in alert *mdx* mice

A total of 148 PC (100 in *mdx* and 48 in WT) were recorded and analyzed in nine *mdx* and eight WT mice. Figure 1 illustrates examples of typical extracellular recordings of PC (left) and corresponding autocorrelograms (right) in two controls (Figure 1(a,b)) and two *mdx* mice (Figure 1(c,d)). Spontaneous SS firing rate was significantly higher in *mdx* mice ( $104.9 \pm 59$  Hz in *mdx* mice vs.  $67.3 \pm 29.9$  Hz in control mice,  $p < 0.001$ ) (Wilcoxon Mann–Whitney test) (Figure 1(e)). PC firing recorded in *mdx* mice was also more regular, as demonstrated by the significantly decreased CV ( $0.20 \pm 0.11$  in *mdx* mice vs.  $0.34 \pm 0.20$  in control mice,  $p < 0.0001$ ) (Wilcoxon Mann–Whitney test) (Figure 1(f)). This was accompanied by a significant increase in SS firing rhythmicity, as illustrated by the SS autocorrelograms presenting numerous side peaks in *mdx* mice (Figure 1(c,d), right) in comparison to the flat autocorrelogram in control mice (Figure 1(a,b), right). This effect was quantified by the RI, showing a significant increase ( $p < 0.0001$ ) (Wilcoxon Mann–Whitney test) in *mdx* ( $0.29 \pm 0.36$ ) compared to control mice ( $0.08 \pm 0.06$ ) (Figure 1(g)).

### 4.2 | Post-CS pause is longer in *mdx* mice

CS firing rate was similar in both groups ( $0.9 \pm 0.4$  Hz in *mdx* mice vs.  $0.9 \pm 0.3$  Hz in control mice,  $p > 0.05$ ) (Figure 2(a)). The CS mean duration was longer in *mdx* mice ( $9.5 \pm 2.8$  ms in *mdx* mice vs.  $8.6 \pm 1.6$  ms in control mice) but the difference was not significant (Figure 2(b)) and CS were followed by a significantly longer pause in SS firing in *mdx* mice ( $14.69 \pm 5.23$  ms in *mdx* mice vs.  $11.65 \pm 2.43$  ms in control mice,  $p < 0.0001$ ) (Wilcoxon Mann–Whitney test) (Figure 2(c)).

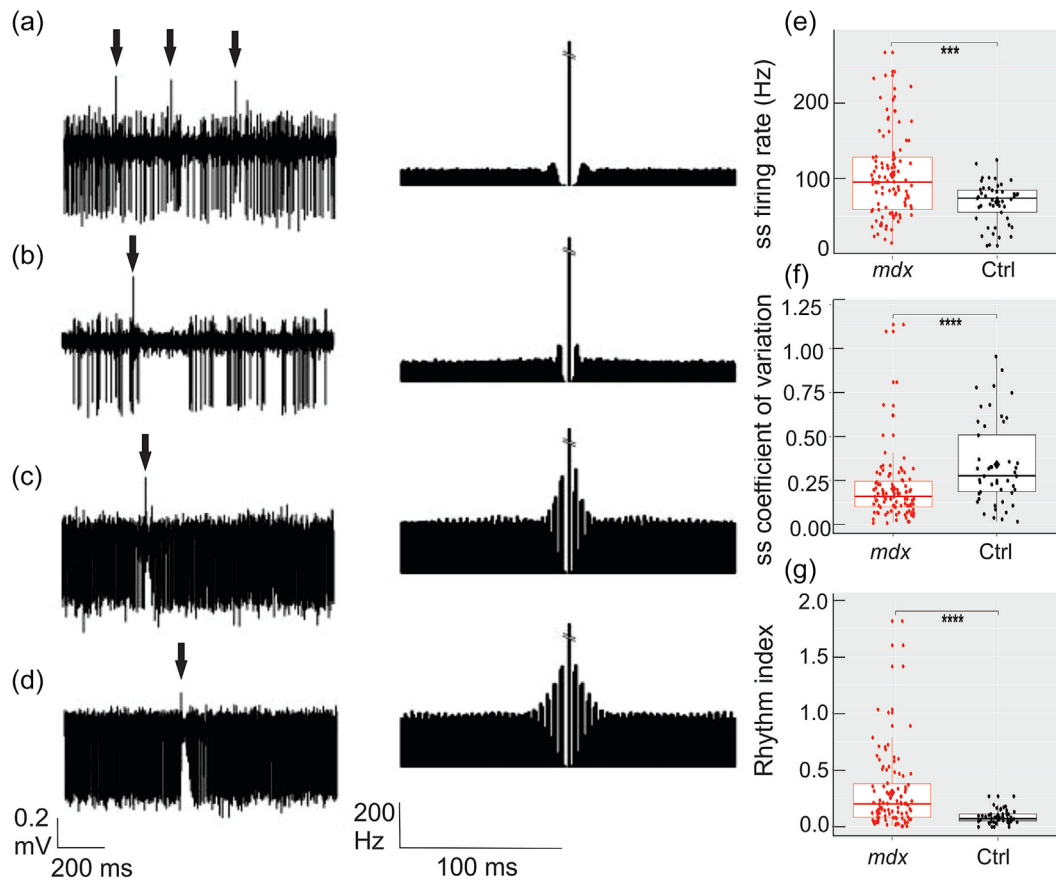


**FIGURE 1** Purkinje cells firing is altered in *mdx* mice. Representative extracellular recordings (left) of a Purkinje cell in two control (a, b) and two *mdx* (c, d) mice with corresponding simple spikes autocorrelograms computed on a 120-s sample (right). Arrows indicate complex spikes (CS). Central peak artifacts in the autocorrelograms were shortened. Box plots of simple spikes (SS) firing rate (e), coefficient of variation (CV) (f) and rhythm index (g) in control (Ctrl) ( $n = 48$ ) and in *mdx* ( $n = 100$ ) Purkinje cells. Bars indicate standard deviation (in this figure and in the following ones, \* $p < 0.05$ ; \*\* $p < 0.01$ , \*\*\* $p < 0.001$ ; \*\*\*\* $p < 0.0001$ ) (Wilcoxon Mann–Whitney test). *mdx*, muscular dystrophy X-linked mouse.

### 4.3 | *mdx* mice present fast LFP oscillation in the cerebellar cortex

Given the increased rhythmicity of PC in *mdx* mice, we investigated the presence of LFP oscillation (LFPO) (Cheron et al., 2004). All *mdx* mice ( $n = 9$ ) presented fast (~160–200 Hz) LFPO, reaching maximal amplitude close to the PC layer (Figure 3(a)), in all explored parts of the cerebellum, whereas none of the control mice ( $n = 8$ ) did. Recordings of LFPO at various depths of the cerebellar cortex (50–400  $\mu\text{m}$ ) in an *mdx* mouse and corresponding FFT analysis are illustrated in Figure 3(b). Fast LFPO amplitude increased progressively as the electrode approached the PC layer, reaching maximal amplitude close to the PC layer (depth 200  $\mu\text{m}$ ). Fast LFPO disappeared at 300  $\mu\text{m}$ , a depth corresponding to the granular cells layer. The fast LFPO was not constant throughout the recordings but occurred as spindle-shaped episodes of oscillations (maximal amplitude  $0.35 \pm 0.10$  mV) with a

mean rate of occurrence of  $8.5 \pm 2.0$  episodes per second. FFT analysis demonstrated a main frequency of  $194.6 \pm 47.2$  Hz (Figure 3(b)). For highlighting the difference of LFPO power in *mdx* versus WT mice, we illustrated in eight mutants (Figure 4(a)) and eight WT (Figure 4(b)) mice the LFPO FFT histogram recorded in the PC layer level showing that the power of 200 Hz LFPO were more than 16 times stronger in *mdx* mice.

### 4.4 | Cerebellar LTD is altered in alert *mdx* mice

To assess whether the LTD abnormalities observed in cerebellar slices (Knuesel et al., 1999) also occurred in vivo, we applied to alert *mdx* mice a previously described cerebellar LTD protocol (Márquez-Ruiz & Cheron, 2012). LFP evoked responses in WT (Figure 5(a)) upper traces) and *mdx* mice (lower traces) demonstrated

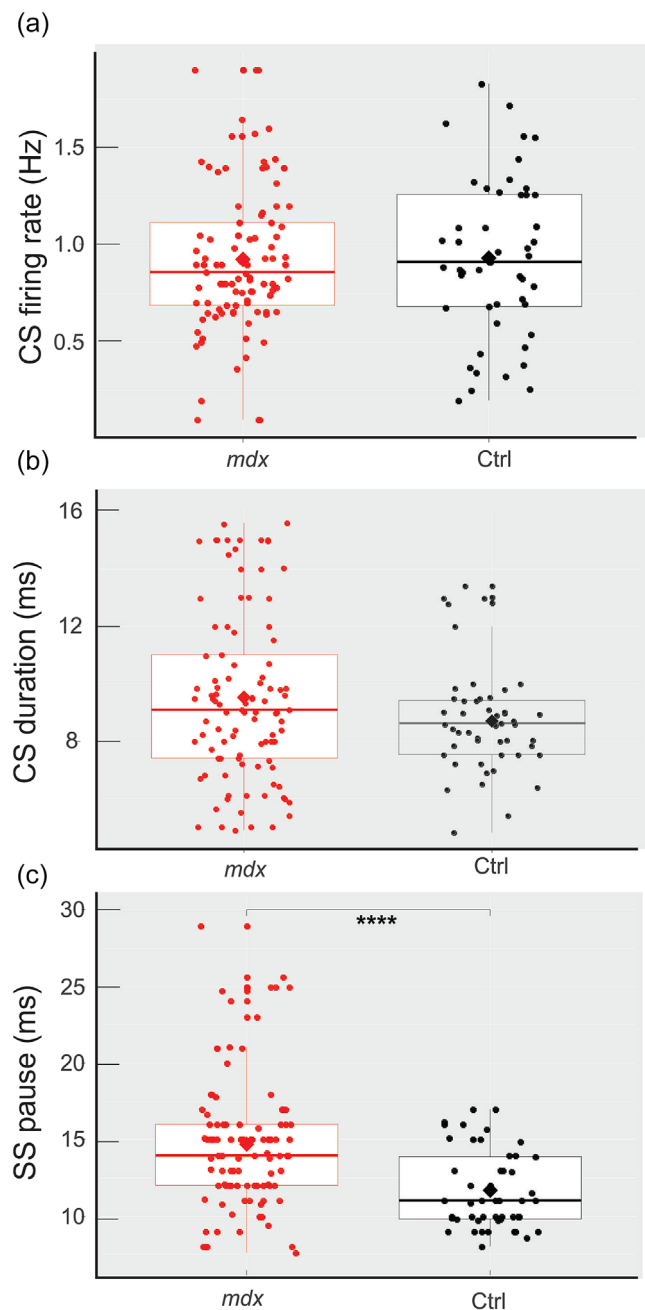


**FIGURE 2** Box plot graphs of complex spikes (CS) firing rate (a), duration (b) and SS pause (c) in control (Ctrl) ( $n = 48$ ) and in *mdx* ( $n = 100$ ) Purkinje cells. Bars indicate standard deviation. SS, simple spikes.

the classical N1-N2-N3 evoked components before (black traces) and after the 8-Hz stimulation (red traces), where N1 reflects presynaptic input and N2 and N3 reflect the postsynaptic response at the recording site (Figure 5(b), upper black trace).

Following 10 min of the 8-Hz stimulation, the latencies of the N2 and N3 peaks increased in WT mice (Figure 5(b), upper red trace) and a marked decrease in the amplitude of the N3 component was observed (see

\* in Figure 5(b) upper red trace). This effect was maximal just after conditioning ( $\sim 50\%$  amplitude decrease) and lasted for over 30 min. In contrast, no significant change in N1 or N2 amplitude was observed upon conditioning.

Mean LFP amplitude (Figure 5(c–e)) and latency changes (Figure 5(d–f)) were quantified for each of the LFP components (N1: black trace, N2: blue trace, and N3: red trace) by comparing averages over each 5-min interval before and after the 8-Hz stimulation protocol. The LTD effect on the N3 amplitude present in WT mice (Figure 5(b,c)) was absent in *mdx* mice (Figure 5(e)). In contrast, the LTD effect on N2 and N3 latencies remained present but in a less extent in *mdx* mice (Figure 5(d,f)), indicating that plasticity of the timing shift of these responses was conserved.

#### 4.5 | Calcium-binding protein expression is normal in the cerebellum of *mdx* mice

To test whether the LFPO is related to abnormal expression of calcium-binding proteins whose deletion induces similar LFPO (Cheron et al., 2004), we performed immunofluorescence staining and PCR of the cerebellum for calbindin, parvalbumin and calretinin. Calretinin is expressed in Golgi, Lugaro and unipolar brush cells. Calbindin D-28 K (Cb) is present only in PC; however, parvalbumin (Pv) is present in both molecular interneurons and PC (Schwaller et al., 2002). The level of expression of these three proteins was not different in the cerebellum of *mdx* and WT mice (Figure 6(a)).

#### 4.6 | *mdx* mice display deficits in motor coordination and balance skills

Given the predominant expression of dystrophin in PC and the observed alterations of PC activity in *mdx* mice, we evaluated different motor function tests to assess whether motor force, coordination and balance were impaired in these mice.

*mdx* mice did not exhibit any obvious behavioural alterations when observed under standard housing conditions. During the wire test, *mdx* mice lost their grip much faster than WT mice ( $20 \pm 9$  s in *mdx* mice vs  $48 \pm 15$  s in control mice,  $p < 0.001$ ). In contrast, on the accelerating rotarod, the latency to fall was not significantly different in *mdx* mice compared to controls ( $p > 0.05$ , one-way ANOVA and  $p > 0.05$  for the parameter genotype and interaction genotype-day, two-way ANOVA) (Figure 7(a)). Both groups improved their performance with time, suggesting the absence of motor learning impairment in



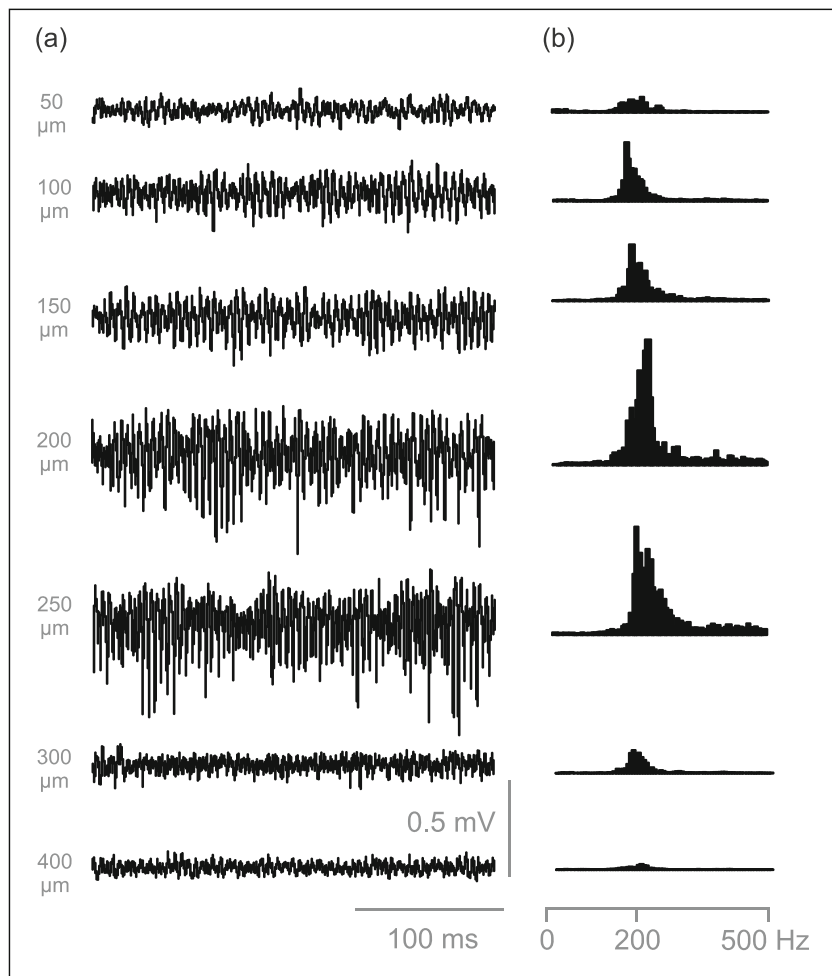


**FIGURE 3** Spatial mapping of LFPO at various depths of the cerebellar cortex (50–400  $\mu\text{m}$ ) in an *mdx* mouse (a) and a representative successive LFPO FFT analysis recorded along a track performed around the PC layer (b). FFT histograms of the LFPO signals recorded at the corresponding depth along the track. The same LFPO profile was reproduced around the PC layer identified by PC recording; only the first 500 Hz is illustrated. FFT, fast Fourier transform; LFPO, local field potential oscillation; *mdx*, muscular dystrophy X-linked mouse; PC, Purkinje cell.

*mdx* mice for this task ( $p < 0.005$  for the parameter day, two-way ANOVA). In the runway test, *mdx* mice made significantly more slips, although their performance improved significantly over time [two-way ANOVA (days 1–5): genotype  $p < 0.005$ , day  $p < 0.005$ , interaction genotype-day] (Figure 7(b)) (Student's *t*-test  $p < 0.05$ ; J1–J4 mais NS J5 et J12, Bonferonni NS). However, the time to go across the runway was not significantly different between control and *mdx* mice and there were no falls in either group (data not shown). The analysis of the retention tests, carried out a week (Figure 7) or 2 months (data not shown) after the last training session, did not reveal any significant difference in performance between the two groups ( $p > 0.05$ , two-way ANOVA and Bonferonni), suggesting that motor learning ability is not impaired in *mdx* mice. The Catwalk test showed a significant widening of the base of support between the forelimbs in *mdx* mice ( $13.03 \pm 1.02$  mm in *mdx* mice vs.  $11.49 \pm 0.71$  mm in WT mice,  $p < 0.01$ , Student's *t*-test) (Figure 7(c)) and between the hindlimbs ( $23.73 \pm 0.81$  mm in *mdx* mice vs.  $21.77 \pm 2.12$  mm in control mice,  $p < 0.01$ , Student's *t*-test) (Figure 7(d)). Altogether,

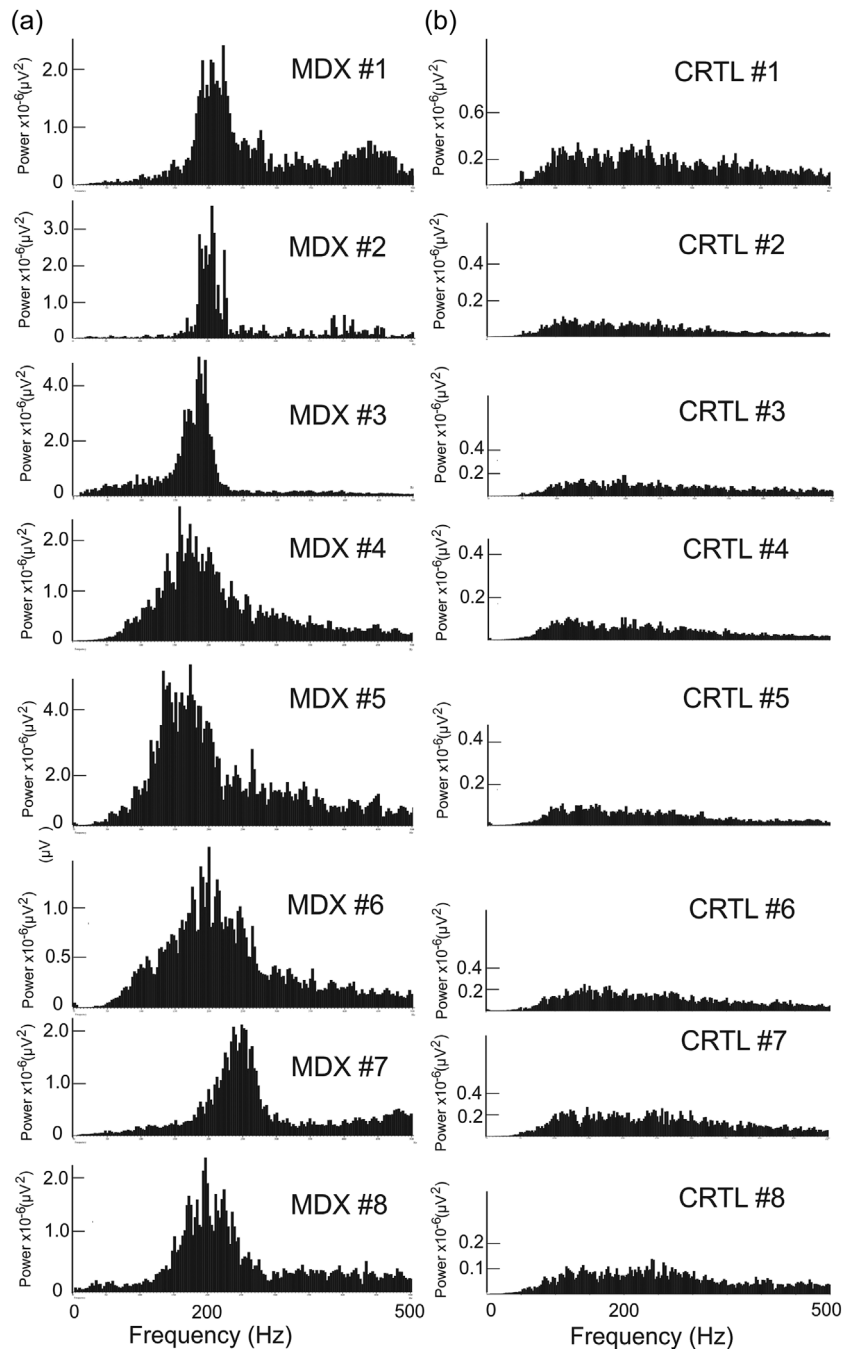
these results indicate impaired force, motor coordination and balance skills in *mdx* without motor learning ability impairment.

## 5 | DISCUSSION

### 5.1 | Motor coordination and learning

As regards motor function, the significant weakness of the *mdx* mice in the wire test contrasts with the maintenance of performance in the accelerating rotarod test. However, both tests can be influenced not only by muscle force weakness well recognized in the absence of dystrophin but can also be significant in case of gait problems or just in case of obesity. Extreme fatigue was also reported in *mdx* mice that may influence all the behavioural testing. We cannot make direct causal relationships between the impairment revealed by the different behavioural testing and the electrophysiological alteration of the PC, because muscle force weakness while present (see the wire test) was not generalized to other

**FIGURE 4** FFT histograms of 200 Hz LFPO recorded in eight mdx (a) and eight control mice, Ctrl (b). Notice the smaller power values and wider frequency spectrum for control vs. mdx mice. FFT, fast Fourier transform; LFPO, local field potential oscillation; mdx, muscular dystrophy X-linked mouse.



behavioural tests and because functional compensation which may occur outside of the cerebellum cortical network in the mutant. However, the impairments reported during the runway and the catwalk test are consistent with cerebellar dysfunction and in accordance with previous studies reporting impairments in motor function in *mdx* mice, including balance (Grady et al., 2006), righting reflex and negative geotaxis (Rafael et al., 2000). Moreover, ataxia has been reported in older *mdx* mice (Bulfield et al., 1984). In contrast, performance on the accelerating rotarod was not significantly different in *mdx* mice compared to their controls. *mdx* mice

improved their performance with time, suggesting effective motor learning and retention tests did not demonstrate defects in memory.

## 5.2 | Electrophysiological alteration of *mdx* PC

Since PC constitutes the sole output of the cerebellar cortex, the regulation of their firing is crucial for cerebellar function, and PC alterations are expected to have repercussions in diverse functions controlled by the

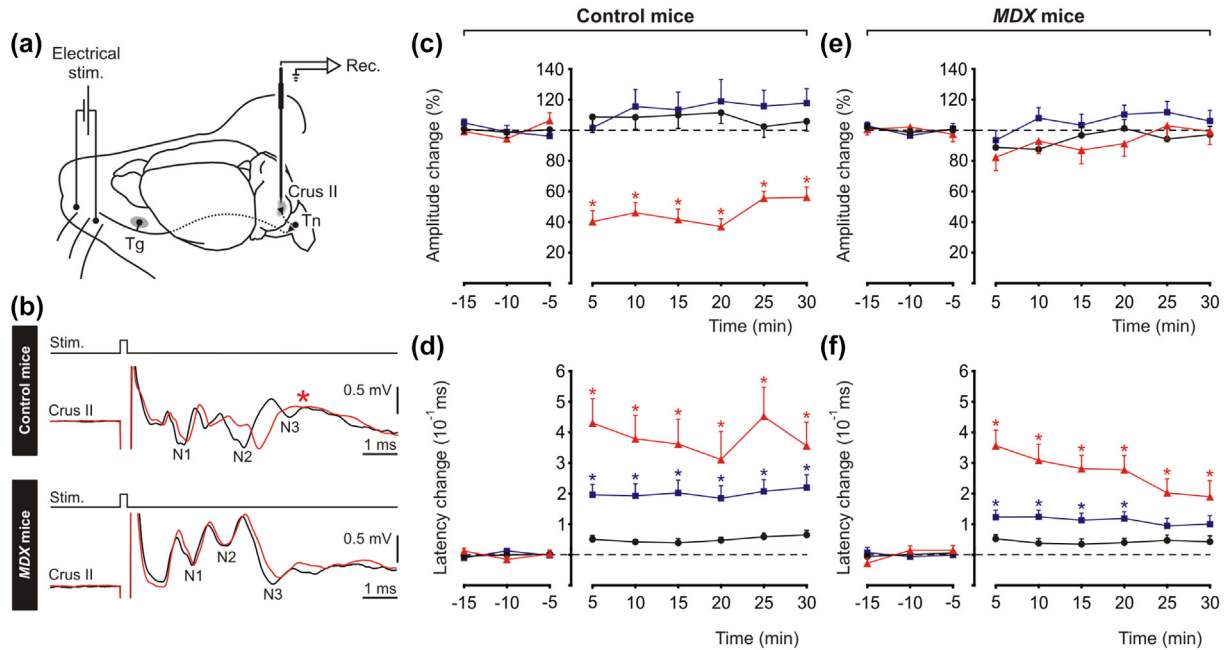


**FIGURE 5** Experimental design and LFP response to electrical stimulation of mouse whiskers and changes in cerebellar LTD in alert mice. (a) Facial dermatomes of the whisker region were electrically stimulated with a pair of needles under the skin. Sensory information comes into the Crus II area from the trigeminal nucleus (Tn) in the brainstem, which receives afferent signals from the trigeminal ganglion (Tg). (b) Early response associated with sensory input in the cerebellum via the trigeminal nucleus is characterized by N1–N2–N3 components. Averaged superimposed traces of the evoked field potential components before the 8-Hz stimulation protocol (black trace) and 30 min after the 8-Hz stimulation protocol (red trace) in control (top) and in *mdx* mice (bottom). The red star indicates the decrease of the N3 amplitude after the 8-Hz stimulation in control mice. The time course of N1 (black trace), N2 (blue trace) and N3 (red trace) amplitude (c–e) and latency (d–f) changes before (negative periods) and after (positive periods) the 8-Hz stimulation protocol (not shown) in four *mdx* ( $n = 27$ ) and five WT mice ( $n = 15$ ). Mean normalized data represent the peak amplitude of the different components calculated for each 5-min interval (c–e) and the time difference at peak latency between each 5-min interval and the mean value measured in control conditions (d–f). Data points are mean  $\pm$  SEM. Significant differences between *mdx* and control mice are indicated with asterisks (Student's *t*-test,  $*p < 0.05$ ). LFP, local field potential; LTD, long-term depression; *mdx*, muscular dystrophy X-linked mouse; SEM, standard error of the mean.

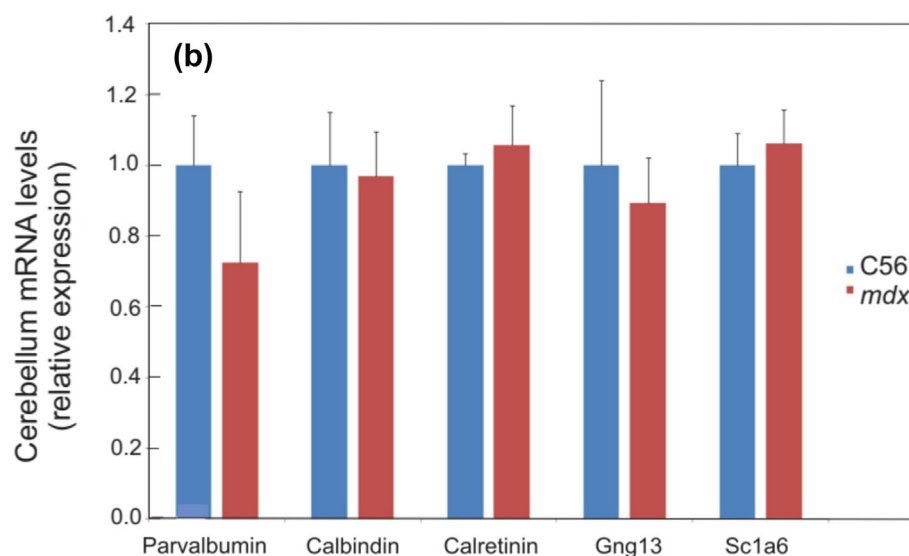
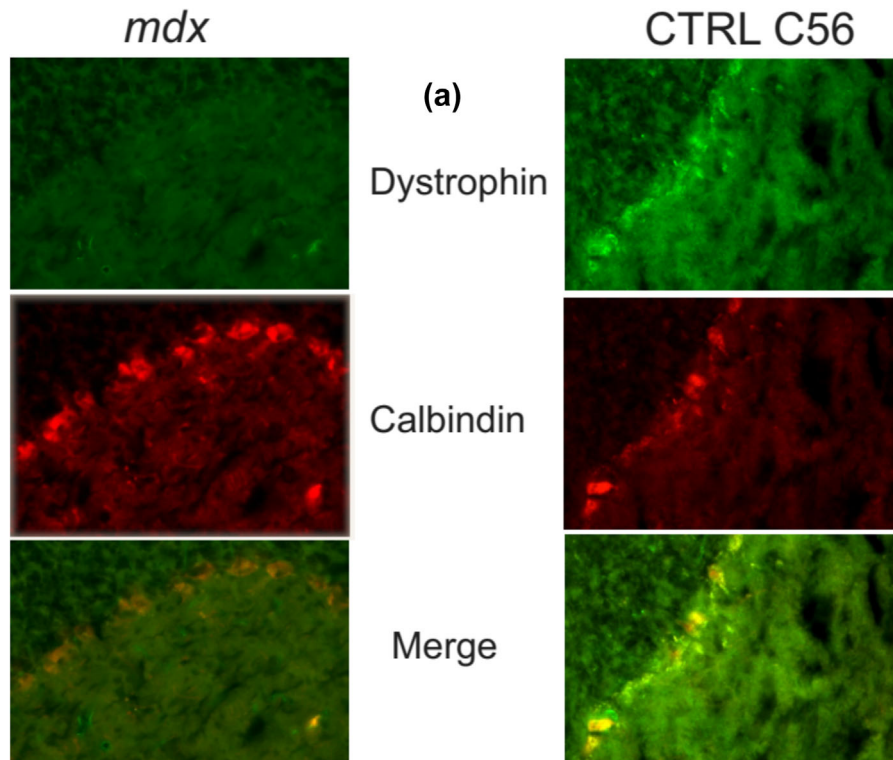
cerebellum. The fact that the basic cytoarchitecture of the different cell layers of the *mdx* mice cerebellum is well-preserved and that the inhibitory neurons presented the same regional organization as those in control mice (Stay et al., 2019) allowed us to focus on the functional aspect of PC.

Adult SS discharges of the PC represents the integration of four main influences: (1) the pacemaker intrinsic activity (Häusser & Clark, 1997), (2) the GABAergic synaptic signals from molecular interneurons (MLI) (basket and stellate cell), (3) the glutamatergic synaptic signals from the parallel fibres and (4) the CS signalling from the climbing fibre. Concerning the first factor, there is only one patch-clamp study on dissociated PC (Snow et al., 2014) available which failed to demonstrate a significant difference in cell capacitance, input resistance, action potential threshold and action potential slope, between *mdx* and control. This may indicate that the pacemaker intrinsic activity factor is not altered. In contrast, this study reported that spontaneous PC firing was

lower in vitro *mdx* PC in the lateral part of the cerebellum but not in the vermal region.

Electrophysiological results showed that SS firing rate, regularity and rhythmicity were significantly increased in alert *mdx* mice. Our group previously demonstrated that mice lacking calcium-binding proteins have increased SS rhythmicity and synchronicity that may sustain the emergence of fast LFPO (Cheron et al., 2004). Given the increased rhythmicity of PC in *mdx* mice, we investigated the presence of LFP oscillations, and we found that SS increased firing rate and enhanced rhythmicity in *mdx* mice were also associated with the emergence of fast LFPO ( $\sim 160$ – $200$  Hz) in the cerebellar cortex of alert *mdx* mice. In accordance with our previous studies on fast pathological LFPO (Cheron et al., 2004, 2005; Servais et al., 2005, 2007; Sicot et al., 2017), we here showed that the PC populations appear to be the major generator of the fast LFP oscillations, as suggested by the depth recording profile (Figure 3) and by previous findings demonstrating

**FIGURE 6** Quantification of three major calcium-binding proteins in the cerebellum. Co-immunofluorescence detection of dystrophin (green) and calbindin protein (red) on sagittal sections of cerebellum of C57 and *mdx* mice (a). Immunofluorescence detection of dystrophin, calbindin and co-expression of dystrophin and calbindin in sagittal sections of cerebellum of C57 and *mdx* mice (b). Expression levels of parvalbumin, calbindin, and calretinin were not significantly different between C57 and *mdx* mice (the parvalbumin and calretinin were not illustrated). Gng13 and Sc1a6 expression levels were used as specific markers of PC (c). Results are mean  $\pm$  SEM (three to four mice per group). Statistical analyses were performed using Student's *t*-test. Statistical significance was set at  $p < 0.05$ . *mdx*, muscular dystrophy X-linked mouse; SEM, standard error of the mean.



synchronization between fast LFPO and both SSs and CSs, and LFPO synchronization along the parallel fibre beam (Cheron et al., 2004).

Among the other factors, the alteration of the GABAergic synaptic signalling presents itself as the first candidate explaining the increase of the SS firing in alert *mdx* mice. In vivo PC discharge spontaneously at a highly irregular rate and are poorly rhythmic in alert animals (Cheron et al., 2004, 2005; Goossens et al., 2001). Although the functional meaning of the irregular spontaneous discharge in PC is not known yet, a theoretical study has suggested that it helps PC to respond rapidly,

sensitively and linearly to external inputs (van Vreeswijk & Sompolinsky, 1996). Therefore, the increased firing rate and enhanced regularity and rhythmicity of SS discharge in alert *mdx* mice would induce a less adaptable and flexible PC response. The highly regular, rhythmic firing pattern of PC suggests a functional disorganization of the cerebellar cortex in *mdx* mice. PC appears to be 'trapped' in stereotyped, non-adaptable firing. It was demonstrated (Häusser & Clark, 1997) that this irregular discharge is not caused by excitatory synaptic drives but by tonic influences from inhibitory interneurons. They also demonstrated that blockade of

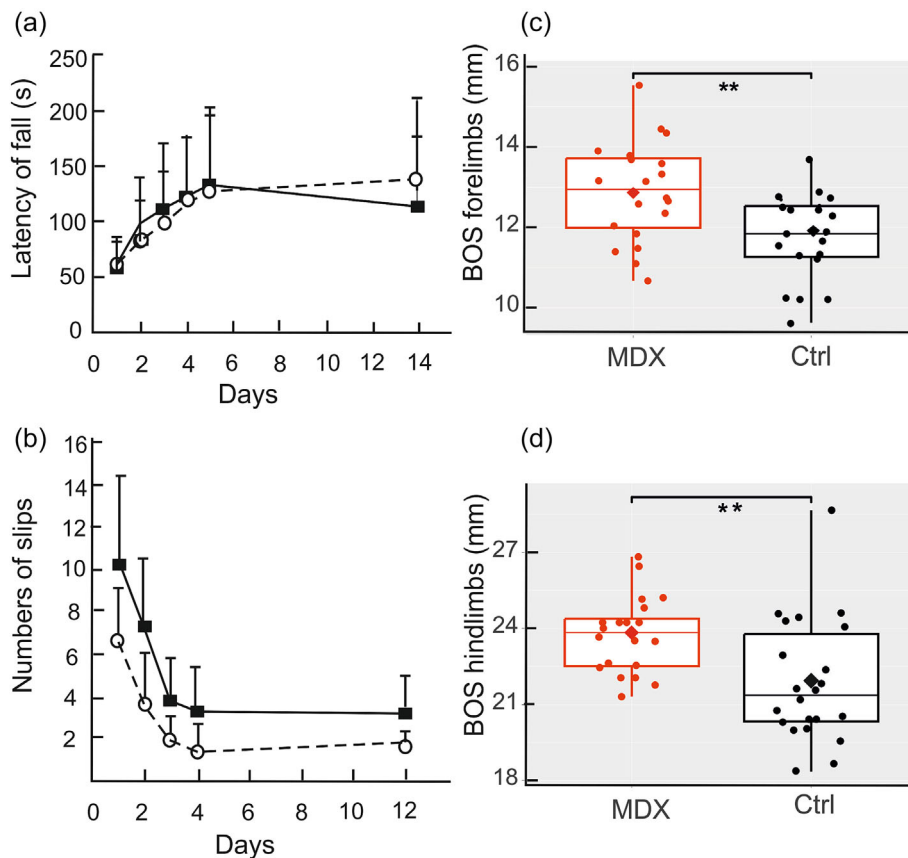


**FIGURE 7** Mdx mice display mild impairment in motor coordination and balance skills. (a) Accelerating rotarod test (two-way ANOVA,  $p > 0.05$ ). (b) Runway test (two-way ANOVA,  $p < 0.005$ , \*\*\*). Behavioral tests were performed on  $n = 10$  mdx and  $n = 11$  WT. Data points are mean  $\pm$  SD. (a) Accelerating rotarod showing no significant difference in latency to fall in mdx mice compared to their controls ( $p > 0.05$ , one-way ANOVA, and  $p > 0.05$  for the parameters genotype and interaction genotype-day, two-way ANOVA) and improvement of performance over time in both groups, suggesting the absence of motor learning impairment in mdx mice ( $p < 0.005$  for the parameter day, two-way ANOVA). (b) Runway test: mdx mice (black square) made significantly more slips, although their performance improved significantly over time (two-way ANOVA [days 1–5]: genotype  $p < 0.005$ , day  $p < 0.005$ , interaction genotype-day). (c, d) Box plots of the catwalk test (BOS, basis of support; Student's *t*-test,  $p < 0.01$ , \*\*). ANOVA, analysis of variance; mdx, muscular dystrophy X-linked mouse; SD, standard deviation; WT, wild type.

somatic GABAA receptors in PC can cause slight depolarization of membrane potential and concomitant increases in action potential regularity and frequency. Further, focal application of GABA to Purkinje neuron somata results in membrane hyperpolarization and diminished spontaneous firing (Okamoto et al., 1983).

In agreement with this, we demonstrate that the loss of dystrophin and the possible (see below) decreased inhibitory drive significantly increases the rate, regularity and rhythmicity of PC SS discharge. Surprisingly, Stay et al. (2019) reported a small decrease of the SS firing and an increase of irregularity in *mdx* mice. Despite a clear demonstration of a reduction in the inhibitory input of MLIs on the PC of *mdx* mice, Wu et al. (2022) do not observe a significant difference in the basal firing frequency of PC but show a greater amplitude excitatory response of CP during sensory stimulation. The presence

of an important overlapping between the study of Stay et al. (2019) (lobules VI–VII), the one of Wu et al. (2022) (Crus I–II and VI–VII lobules) and the present study (Crus I–II and IV–VIII/IXa and IXb lobules) cannot entirely explain these discrepancies. These can be partly explained by other factors such as the fact that female mice were used in Stay et al. (2019) but only male were used in Wu et al. (2022) and in the present case. The brain state of the awake mice during the recording can be a more potent factor. For example, the recording was made in some experiments on the first day, more than 1 h after the surgery in Wu et al. (2022) and at least 1 day after the surgery in the present case. The behavioural condition was not the same, the mice were placed on a foam wheel allowing free movements of the four limbs in Wu et al. (2022) while in our case, the mice were placed in a soft plastic tube restraining the limb movements.

Another factor could be linked to the type of electrode; high-electrode density silicon probe was used by Wu et al. (2022) and tungsten Eckhorn electrode in Stay et al. (2019) and in the present study.

Empson et al. (2013) demonstrated that an enhancement of the MLI activity effectively reduced the frequency and the regularity of the PC of PMCA2 knockout mice presenting ataxia. At the opposite, the dysfunctional signalling at GABA synapses on PC due to the loss of dystrophin (PC) causing destabilization of GABA<sub>A</sub> receptor clustering (Chamberlain et al., 1988; Knuesel et al., 1999; Nudel et al., 1988; Zarrouki et al., 2022) and the increased rate of [3H]-GABA uptake in synaptosomes of *mdx* PC as reported by Pereira da Silva et al. (2018) would logically induce a disinhibition of the *mdx* PC explaining the SS firing increase and the emergence of the fast LFPO.

In favour of this possibility, when GABA(A) antagonist bicuculline was infused into the slice, the amplitude of the miniature IPSCs was less in *mdx* PC than in control, and more indirectly, the increase in EPSP amplitude in the presence of bicuculline was also less than in control (Anderson et al., 2003). The decrease of the miniature IPSC in *mdx* PC was confirmed by Kueh et al. (2008). These authors also demonstrated later (Kueh et al., 2011) that if the number of receptors at the PC GABAergic synapses was importantly reduced in *mdx* PC, they functioned normally. However, they also demonstrated by infusion of gaboxadol (an agonist of extra-synaptic GABA<sub>A</sub> receptors) a reactive increase of the number of extra-synaptic GABA<sub>A</sub> receptor gaboxadol in this mutant. The fact that the holding current was also increased in the *mdx* PC (65 pA in *mdx* versus 37 pA in control) in the presence of gaboxadol (Kueh et al., 2011) moderates the possibility that the present SS frequency increase in *mdx* PC was mainly due to a reduced inhibition.

Surprisingly, whole-cell recording performed in urethane-anaesthetized mice (Jin et al., 2017) demonstrated that the application of gabazine (GABA<sub>A</sub> receptors antagonist) did not modify the SS firing rate. In contrast, an AMPA receptor blocker abolished CS activity and induced significantly increased SS firing rates and a decreased CV SS value.

In addition to a role in GABA<sub>A</sub> receptor anchoring and clustering, dystrophin forms a multi-protein dystrophin-associated glycoproteins complex (DGC) in the CNS similar to that seen in muscle (Waite et al., 2009). In brain tissue, components of the DGC, including dystrophin, interact with several ion channels, such as voltage-gated Na<sup>+</sup> channels (Gee et al., 1998) and inward rectifier K<sup>+</sup> channels (Connors et al., 2004), and are implicated in stabilizing multiple ion channels that are crucial to PC excitability.

As CS directly reflects the firing activity of olivary neurons, the conserved CS firing rate in *mdx* mice suggests that the cerebello-olivary loop is not altered in *mdx* mice. In the same line, as it was demonstrated that the duration of the pause in SS, triggered by the CS, depends on the PC dendritic spikes (Davie et al., 2008), the present increase of the pause duration may indicate a conserved action of the dendritic spikes of the *mdx* PC.

### 5.3 | Dystrophin and calcium homeostasis

Several elements point out the role of dystrophin in calcium homeostasis. In dystrophic muscle tissue, the loss of dystrophin and its associated DGC leads to increased intracellular Ca<sup>2+</sup> levels that contribute to its pathology (Whitehead et al., 2006). The PC activity is strongly regulated through the mossy fibre and olivocerebellar systems (Welsh et al., 1995) and through dynamic mechanisms involving intracellular Ca<sup>2+</sup> fluxes (Llinás & Sugimori, 1980). In the *mdx* mouse sensorimotor cortex, the number of neurons positive for the cytosolic Ca<sup>2+</sup>-buffer, calbindin, is increased relative to controls (Carretta et al., 2003).

Concerning the presence of dystrophin in the granular layer (Nicchia et al., 2008), Haws and Lansman (1991) reported that Ca<sup>2+</sup>-channel kinetics are aberrant in *mdx* granule cells, as channels remain open substantially longer than in WTs (Haws & Lansman, 1991). Furthermore, Steinhardt's group used Ca<sup>2+</sup>-sensitive dyes to demonstrate that resting Ca<sup>2+</sup> level was elevated in cultured *mdx* granular cells (Hopf & Steinhardt, 1992). This is in agreement with the increase in calcium-positive neurons reported in the *mdx* mice (Tuckett et al., 2015) and could lead to an increased intrinsic excitability of the afferent granule cells and therefore hurt PC activity. Such a situation has been encountered in calretinin knockout mice where the SS frequency was increased and accompanied as in the present mutant by fast LFPO (Schiffmann et al., 1999). These electrophysiological alterations and related ataxia were restored (Bearzatto et al., 2006) by a selective re-expression of calretinin in granule cells. This indicates that the fine excitability tuning of these cells through the regulation of Ca<sup>2+</sup> homeostasis plays a crucial role in the final integrative function exerted by the PC. However, a same scenario with a deficit in calcium-binding proteins seems unlikely in the present case because we did not demonstrate any significant difference in the expression of the three major calcium-binding proteins, namely parvalbumin, calbindin and calretinin proteins in the cerebellum of *mdx* mice compared to controls (Cheron et al., 2004). However, to exclude Ca<sup>2+</sup>

homeostasis implication, extended investigations will be needed.

#### 5.4 | Impairment of LTD and increasing of CS duration and SS pause

In contrast to the conserved CF functions in the *mdx* mice, the LTD of the N3 component [originating from the PF-PC synapse (Márquez-Ruiz & Cheron, 2012)] was absent. This alteration is compatible with the absence of in vitro LTD in the same mutant (Anderson et al., 2010). Moreover, another similitude between this in vitro experiment and the present in vivo was the conservation of the presynaptic (before the PF-PC synapse) plasticity reciprocally represented by the preserved paired-pulse facilitation and the preserved N2-N3 timing plasticity in *mdx* mice. In this context, Steuber et al. (2007) have shown with in vitro and modeling approaches that after the LTD induction, the stimulation of the parallel fibre (PF) was able to evoke a delayed timing of the second and the third PC spikes of the evoked burst pattern. In this situation, only the modification at the PF-PC synapses can explain this timing plasticity. This is like the present delayed latencies of the N2-N3 component quite less strong in *mdx* than in WT mice. However, we cannot avoid the possibility that the observed time-delay was due to plasticity at the mossy fibre-GC synapses which was demonstrated in vitro (Mapelli & D'Angelo, 2007) and in the anaesthetized rat (Roggeri et al., 2008). This possibility is theoretically supported from the notion that the mossy fibre-GC synapses, regulated by Golgi cells, make a template for timing adjustments of the mossy fibre input (D'Angelo et al., 2009). Interestingly, the absence of the same type of LTD for both the amplitude of the N3 component and the timing plasticity of N2-N3 in the specific knockout for the BK channels of the PC (Cheron et al., 2018) and the conserved timing plasticity in the present *mdx* mice show that the two types of plastic changes, namely N2-N3 time shift and N3 amplitude decrease, involve different mechanisms. The absence of LTD on N3 amplitude may be explained by an imbalance in PC excitatory inhibitory input altering the LTD process but conserving N2-N3 timing plasticity.

In accordance to the present findings of an increase of the SS pause, Helleringer et al. (2018) demonstrated in selective Dp71knockout mice slice a selective increase of the glutamatergic transmission at the climbing fibre-PC synapses but not at the parallel fibre-PC synapses. This enhanced excitatory drive was associated with deficient synaptic plasticity and alteration of clustering of scaffolding postsynaptic density protein PSD-95. The genetic loss of Dp71 has been associated to intellectual deficiency

(Daoud et al., 2009); Dp71 is the most important dystrophin-gene product in the adult brain and is expressed in both glial and neuronal cells (Nicchia et al., 2008; Tadayoni et al., 2012). The reported expression of Dp71 in the cerebellar Bergmann glial cells is particularly relevant because similar high-frequency (200 Hz) LFPO was found in the cerebellum of DMXL mice (a mouse model of the myotonic dystrophy type 1) in association with abnormal PC firing, RNA toxicity in Bergmann glia and motor incoordination (Sicot et al., 2017). In addition, the same study showed that the membrane transporter (GLT1) mainly expressed by the Bergmann glia to clear glutamate release was downregulated in the DMXL mice, inducing an increased excitation of the PC and the emergence of 200 Hz LFPO as in the present case. We may thus speculate based on Helleringer et al. (2018) and Sicot et al. (2017) studies that defective neuroglial communication remains a possible explanation of the present abnormalities recorded in the *mdx* mice cerebellum. This possibility should be investigated in future investigations.

## 6 | CONCLUSIONS

To our knowledge, we performed the first study in alert *mdx* mice comparing in vivo PC firing and cerebellar LTD. We demonstrated altered PC firing, the emergence of fast LFP oscillations and significant impairment of LTD in *mdx* cerebellar PC in vivo, pointing to an essential role for dystrophin in neuronal responsiveness and connectivity. These findings demonstrate the existence of a cerebellar dysfunction expressed here by impairment during the runway and the catwalk test in *mdx* mice. We hypothesize that similar cerebellar dysfunctions may be present in patients with DMD. Our results support the hypothesis that cognitive deficits associated with DMD could, indeed, be mediated by the loss of dystrophin protein in the central nervous system.

### AUTHOR CONTRIBUTIONS

G. C. and N. D. conceived the original idea; G. C. designed the experiments; G. C., C. P. and J. M. R. performed the experiments. G. C., C. P. and P. G. analyzed the data; G. C. and C. P. wrote the first draft of the manuscript. J. M. R., A. M. C., N. D., L. S. P. G. and B. D. contributed to the writing.

### ACKNOWLEDGEMENTS

The authors would like to thank J. Francq and S. Henuy for providing excellent animal care; M. Dufief, E. Toussaint, T. D'Angelo, E. Hortmanns and M. Petieau for expert technical assistance; O. Shackman for his

assistance with the behavioural testing; D. Ristori for statistical analysis. This work was supported in part by grants from the Fonds National de la Recherche Scientifique (FNRS) (Belgium), Fonds de Recherche de l'Université Libre de Bruxelles (Belgium), Fonds de Recherche de l'Université de Mons (Belgium), from the Brain & Society Foundation (Belgium) and Leibu Fond (Belgium). C. Prigogine was supported by a research fellowship/assistant of the Fonds National de la Recherche Scientifique (FNRS), Belgium.

### CONFLICT OF INTEREST STATEMENT

The authors declare no conflicts of interest.

### DATA AVAILABILITY STATEMENT

All relevant data will be available from the corresponding authors upon request.

### PEER REVIEW

The peer review history for this article is available at <https://www.webofscience.com/api/gateway/wos/peer-review/10.1111/ejn.16566>.

### ORCID

Ana Maria Cebolla  <https://orcid.org/0000-0002-3710-7923>

Guy Cheron  <https://orcid.org/0000-0003-0734-583X>

### REFERENCES

- Amoasii, L., Long, C., Li, H., Mireault, A. A., Shelton, J. M., Sanchez-Ortiz, E., McAnally, J. R., Bhattacharyya, S., Schmidt, F., Grimm, D., Hauschka, S. D., Bassel-Duby, R., & Olson, E. N. (2017). Single-cut genome editing restores dystrophin expression in a new mouse model of muscular dystrophy. *Science Translational Medicine*, 9, 9. <https://doi.org/10.1126/scitranslmed.aan8081>
- Anderson, J. L., Head, S. I., & Morley, J. W. (2003). Altered inhibitory input to Purkinje cells of dystrophin-deficient mice. *Brain Research*, 982, 280–283. [https://doi.org/10.1016/S0006-8993\(03\)03018-X](https://doi.org/10.1016/S0006-8993(03)03018-X)
- Anderson, J. L., Morley, J. W., & Head, S. I. (2010). Enhanced homosynaptic LTD in cerebellar Purkinje cells of the dystrophic MDX mouse. *Muscle & Nerve*, 41, 329–334. <https://doi.org/10.1002/mus.21467>
- Anderson, S. W., Routh, D. K., & Ionasescu, V. V. (1988). Serial position memory of boys with Duchenne muscular dystrophy. *Developmental Medicine and Child Neurology*, 30, 328–333. <https://doi.org/10.1111/j.1469-8749.1988.tb14557.x>
- Avanzino, L., Pelosin, E., Vicario, C. M., Lagravinese, G., Abbruzzese, G., & Martino, D. (2016). Time processing and motor control in movement disorders. *Frontiers in Human Neuroscience*, 10, 631. <https://doi.org/10.3389/fnhum.2016.00631>
- Bearzatto, B., Servais, L., Roussel, C., Gall, D., Baba-Aïssa, F., Schurmans, S., de Kerchove d'Exaerde, A., Cheron, G., & Schiffmann, S. N. (2006). Targeted calretinin expression in granule cells of calretinin-null mice restores normal cerebellar functions. *FASEB Journal*, 20, 380–382.
- Bulfield, G., Siller, W. G., Wight, P. A., & Moore, K. J. (1984). X chromosome-linked muscular dystrophy (mdx) in the mouse. *Proceedings of the National Academy of Sciences of the United States of America*, 81, 1189–1192. <https://doi.org/10.1073/pnas.81.4.1189>
- Carretta, D., Santarelli, M., Vanni, D., Ciabatti, S., Sbriccoli, A., Pinto, F., & Minciacchi, D. (2003). Cortical and brainstem neurons containing calcium-binding proteins in a murine model of Duchenne's muscular dystrophy: Selective changes in the sensorimotor cortex. *The Journal of Comparative Neurology*, 456, 48–59. <https://doi.org/10.1002/cne.10506>
- Chamberlain, J. S., Pearlman, J. A., Muzny, D. M., Gibbs, R. A., Ranier, J. E., Caskey, C. T., & Reeves, A. A. (1988). Expression of the murine Duchenne muscular dystrophy gene in muscle and brain. *Science*, 239, 1416–1418. <https://doi.org/10.1126/science.3347839>
- Cheron, G., Gall, D., Servais, L., Dan, B., Maex, R., & Schiffmann, S. N. (2004). Inactivation of calcium-binding protein genes induces 160 Hz oscillations in the cerebellar cortex of alert mice. *Journal of Neuroscience: the Official Journal of the Society for Neuroscience*, 24, 434–441. <https://doi.org/10.1523/JNEUROSCI.3197-03.2004>
- Cheron, G., Márquez-Ruiz, J., Cheron, J., Prigogine, C., Ammann, C., Lukowski, R., Ruth, P., & Dan, B. (2018). Purkinje cell BKchannel ablation induces abnormal rhythm in deep cerebellar nuclei and prevents LTD. *Scientific Reports*, 8, 4220. <https://doi.org/10.1038/s41598-018-22654-6>
- Cheron, G., Servais, L., Wagstaff, J., & Dan, B. (2005). Fast cerebellar oscillation associated with ataxia in a mouse model of Angelman syndrome. *Neuroscience*, 130, 631–637. <https://doi.org/10.1016/j.neuroscience.2004.09.013>
- Comim, C. M., Ventura, L., Freiberger, V., Dias, P., Bragagnolo, D., Dutra, M. L., Amaral, R. A., Camargo-Fagundes, A. L. S., Reis, P. A., Castro-Faria-Neto, H. C., Vainzof, M., & Rosa, M. I. (2019). Neurocognitive impairment in mdx mice. *Molecular Neurobiology*, 56, 7608–7616. <https://doi.org/10.1007/s12035-019-1573-7>
- Connors, N. C., Adams, M. E., Froehner, S. C., & Kofuji, P. (2004). The potassium channel Kir4.1 associates with the dystrophin-glycoprotein complex via alpha-syntrophin in glia. *The Journal of Biological Chemistry*, 279, 28387–28392. <https://doi.org/10.1074/jbc.M402604200>
- Cotton, S., Voudouris, N. J., & Greenwood, K. M. (2001). Intelligence and Duchenne muscular dystrophy: Full-scale, verbal, and performance intelligence quotients. *Developmental Medicine and Child Neurology*, 43, 497–501.
- Cyrlunik, S. E., & Hinton, V. J. (2008). Duchenne muscular dystrophy: A cerebellar disorder? *Neuroscience and Biobehavioral Reviews*, 32, 486–496. <https://doi.org/10.1016/j.neubiorev.2007.09.001>
- D'Angelo, E., Koekkoek, S. K. E., Lombardo, P., Solinas, S., Ros, E., Garrido, J., Schonewille, M., & De Zeeuw, C. I. (2009). Timing in the cerebellum: Oscillations and resonance in the granular layer. *Neuroscience*, 162, 805–815. <https://doi.org/10.1016/j.neuroscience.2009.01.048>



- Daoud, F., Angeard, N., Demerre, B., Martie, I., Benyaou, R., Leturcq, F., Cossée, M., Deburgrave, N., Saillour, Y., Tuffery, S., Urtizbera, A., Toutain, A., Echenne, B., Frischman, M., Mayer, M., Desguerre, I., Estournet, B., Réveillère, C., Penisson-Besnier, I., ... Chelly, J. (2009). Analysis of Dp71 contribution in the severity of mental retardation through comparison of Duchenne and Becker patients differing by mutation consequences on Dp71 expression. *Human Molecular Genetics*, *18*, 3779–3794. <https://doi.org/10.1093/hmg/ddp320>
- Davie, J. T., Clark, B. A., & Häusser, M. (2008). The origin of the complex spike in cerebellar Purkinje cells. *Journal of Neuroscience: the Official Journal of the Society for Neuroscience*, *28*, 7599–7609. <https://doi.org/10.1523/JNEUROSCI.0559-08.2008>
- Deconinck, N., & Dan, B. (2007). Pathophysiology of duchenne muscular dystrophy: Current hypotheses. *Pediatric Neurology*, *36*, 1–7. <https://doi.org/10.1016/j.pediatrneurol.2006.09.016>
- Donders, J., & Taneja, C. (2009). Neurobehavioral characteristics of children with Duchenne muscular dystrophy. *Child Neuropsychology: a Journal on Normal and Abnormal Development in Childhood and Adolescence*, *15*, 295–304.
- Doorenweerd, N., Mahfouz, A., van Putten, M., Kaliyaperumal, R., T' Hoen, P.A.C., Hendriksen, J.G.M., Aartsma-Rus, A.M., Verschuuren, J.J.G.M., Niks, E.H., Reinders, M.J.T., Kan, H.E., & Lelieveldt, B.P.F. (2017). Timing and localization of human dystrophin isoform expression provide insights into the cognitive phenotype of Duchenne muscular dystrophy. *Scientific Reports*, *7*, 12575. <https://doi.org/10.1038/s41598-017-12981-5>
- Dorman, C., Hurley, A. D., & D'Avignon, J. (1988). Language and learning disorders of older boys with Duchenne muscular dystrophy. *Developmental Medicine and Child Neurology*, *30*, 316–327. <https://doi.org/10.1111/j.1469-8749.1988.tb14556.x>
- Dubowitz, V., & Crome, L. (1969). The central nervous system in Duchenne muscular dystrophy. *Brain: a Journal of Neurology*, *92*, 805–808. <https://doi.org/10.1093/brain/92.4.805>
- Eckhorn, R., & Thomas, U. (1993). A new method for the insertion of multiple microprobes into neural and muscular tissue, including fiber electrodes, fine wires, needles and microsensors. *Journal of Neuroscience Methods*, *49*, 175–179. [https://doi.org/10.1016/0165-0270\(93\)90121-7](https://doi.org/10.1016/0165-0270(93)90121-7)
- Empson, R. M., Huang, H., Nagaraja, R. Y., Roome, C. J., & Knöpfel, T. (2013). Enhanced synaptic inhibition in the cerebellar cortex of the ataxic PMCA2(-/-) knockout mouse. *Cerebellum (London, England)*, *12*, 667–675. <https://doi.org/10.1007/s12311-013-0472-0>
- Fujimoto, T., Stam, K., Yaoi, T., Nakano, K., Arai, T., Okamura, T., & Itoh, K. (2023). Dystrophin short product, Dp71, interacts with AQP4 and Kir4.1 channels in the mouse cerebellar glial cells in contrast to Dp427 at inhibitory postsynapses in the Purkinje neurons. *Molecular Neurobiology*, *60*, 3664–3677. <https://doi.org/10.1007/s12035-023-03296-w>
- Gee, S. H., Madhavan, R., Levinson, S. R., Caldwell, J. H., Sealock, R., & Froehner, S. C. (1998). Interaction of muscle and brain sodium channels with multiple members of the dystrophin family of dystrophin-associated proteins. *Journal of Neuroscience: the Official Journal of the Society for Neuroscience*, *18*, 128–137. <https://doi.org/10.1523/JNEUROSCI.18-01-00128.1998>
- Gómez-Beldarrain, M., García-Moncó, J. C., Rubio, B., & Pascual-Leone, A. (1998). Effect of focal cerebellar lesions on procedural learning in the serial reaction time task. *Experimental Brain Research*, *120*, 25–30. <https://doi.org/10.1007/s002210050374>
- Goossens, J., Daniel, H., Rancillac, A., van der Steen, J., Oberdick, J., Crépel, F., De Zeeuw, C. I., & Frens, M. A. (2001). Expression of protein kinase C inhibitor blocks cerebellar long-term depression without affecting Purkinje cell excitability in alert mice. *Journal of Neuroscience: the Official Journal of the Society for Neuroscience*, *21*, 5813–5823. <https://doi.org/10.1523/JNEUROSCI.21-15-05813.2001>
- Gorecki, D., Geng, Y., Thomas, K., Hunt, S. P., Barnard, E. A., & Barnard, P. J. (1991). Expression of the dystrophin gene in mouse and rat brain. *Neuroreport*, *2*, 773–776. <https://doi.org/10.1097/00001756-199112000-00011>
- Grady, R. M., Wozniak, D. F., Ohlemiller, K. K., & Sanes, J. R. (2006). Cerebellar synaptic defects and abnormal motor behavior in mice lacking alpha- and beta-dystrobrevin. *Journal of Neuroscience: the Official Journal of the Society for Neuroscience*, *26*, 2841–2851. <https://doi.org/10.1523/JNEUROSCI.4823-05.2006>
- Hashimoto, Y., Kuniishi, H., Sakai, K., Fukushima, Y., Du, X., Yamashiro, K., Hori, K., Imamura, M., Hoshino, M., Yamada, M., Araki, T., Sakagami, H., Takeda, S., Itaka, K., Ichinohe, N., Muntoni, F., Sekiguchi, M., & Aoki, Y. (2022). Brain Dp140 alters glutamatergic transmission and social behaviour in the mdx52 mouse model of Duchenne muscular dystrophy. *Progress in Neurobiology*, *216*, 102288. <https://doi.org/10.1016/j.pneurobio.2022.102288>
- Häusser, M., & Clark, B. A. (1997). Tonic synaptic inhibition modulates neuronal output pattern and spatiotemporal synaptic integration. *Neuron*, *19*, 665–678. [https://doi.org/10.1016/S0896-6273\(00\)80379-7](https://doi.org/10.1016/S0896-6273(00)80379-7)
- Haws, C. M., & Lansman, J. B. (1991). Calcium-permeable ion channels in cerebellar neurons from mdx mice. *Proceedings of the Biological Sciences*, *244*, 185–189. <https://doi.org/10.1098/rspb.1991.0068>
- Helleringer, R., Le Verger, D., Li, X., Izabelle, C., Chaussenot, R., Belmaati-Cherkaoui, M., Dammak, R., Decottignies, P., Daniel, H., Galante, M., & Vaillend, C. (2018). Cerebellar synapse properties and cerebellum-dependent motor and non-motor performance in Dp71-null mice. *Disease Models & Mechanisms*, *11*, 11. <https://doi.org/10.1242/dmm.033258>
- Hinton, V. J., De Vivo, D. C., Nereo, N. E., Goldstein, E., & Stern, Y. (2000). Poor verbal working memory across intellectual level in boys with Duchenne dystrophy. *Neurology*, *54*, 2127–2132. <https://doi.org/10.1212/WNL.54.11.2127>
- Hinton, V. J., De Vivo, D. C., Nereo, N. E., Goldstein, E., & Stern, Y. (2001). Selective deficits in verbal working memory associated with a known genetic etiology: The neuropsychological profile of duchenne muscular dystrophy. *Journal of the International Neuropsychological Society*, *7*, 45–54. <https://doi.org/10.1017/S1355617701711058>
- Hinton, V. J., Fee, R. J., Goldstein, E. M., & De Vivo, D. C. (2007). Verbal and memory skills in males with Duchenne muscular dystrophy. *Developmental Medicine and Child Neurology*, *49*, 123–128. <https://doi.org/10.1111/j.1469-8749.2007.00123.x>

- Hopf, F. W., & Steinhardt, R. A. (1992). Regulation of intracellular free calcium in normal and dystrophic mouse cerebellar neurons. *Brain Research*, 578, 49–54. [https://doi.org/10.1016/0006-8993\(92\)90228-2](https://doi.org/10.1016/0006-8993(92)90228-2)
- Jin, X.-H., Wang, H.-W., Zhang, X.-Y., Chu, C.-P., Jin, Y.-Z., Cui, S.-B., & Qiu, D.-L. (2017). Mechanisms of spontaneous climbing fiber discharge-evoked pauses and output modulation of cerebellar Purkinje cell in mice. *Frontiers in Cellular Neuroscience*, 11, 247. <https://doi.org/10.3389/fncel.2017.00247>
- Jung, D., Pons, F., Léger, J. J., Aunis, D., & Rendon, A. (1991). Dystrophin in central nervous system: A developmental, regional distribution and subcellular localization study. *Neuroscience Letters*, 124, 87–91. [https://doi.org/10.1016/0304-3940\(91\)90828-H](https://doi.org/10.1016/0304-3940(91)90828-H)
- Kim, T. W., Wu, K., & Black, I. B. (1995). Deficiency of brain synaptic dystrophin in human Duchenne muscular dystrophy. *Annals of Neurology*, 38, 446–449. <https://doi.org/10.1002/ana.410380315>
- Knuesel, I., Mastrocola, M., Zuellig, R. A., Bornhauser, B., Schaub, M. C., & Fritschy, J. M. (1999). Short communication: Altered synaptic clustering of GABAA receptors in mice lacking dystrophin (mdx mice). *The European Journal of Neuroscience*, 11, 4457–4462. <https://doi.org/10.1046/j.1460-9568.1999.00887.x>
- Kueh, S. L. L., Dempster, J., Head, S. I., & Morley, J. W. (2011). Reduced postsynaptic GABAA receptor number and enhanced gaboxadol induced change in holding currents in Purkinje cells of the dystrophin-deficient mdx mouse. *Neurobiology of Disease*, 43, 558–564. <https://doi.org/10.1016/j.nbd.2011.05.002>
- Kueh, S. L. L., Head, S. I., & Morley, J. W. (2008). GABA (a) receptor expression and inhibitory post-synaptic currents in cerebellar Purkinje cells in dystrophin-deficient mdx mice. *Clinical and Experimental Pharmacology & Physiology*, 35, 207–210. <https://doi.org/10.1111/j.1440-1681.2007.04816.x>
- Leibowitz, D., & Dubowitz, V. (1981). Intellect and behaviour in Duchenne muscular dystrophy. *Developmental Medicine and Child Neurology*, 23, 577–590. <https://doi.org/10.1111/j.1469-8749.1981.tb02039.x>
- Lidov, H. G., Byers, T. J., & Kunkel, L. M. (1993). The distribution of dystrophin in the murine central nervous system: An immunocytochemical study. *Neuroscience*, 54, 167–187. [https://doi.org/10.1016/0306-4522\(93\)90392-S](https://doi.org/10.1016/0306-4522(93)90392-S)
- Lidov, H. G., Byers, T. J., Watkins, S. C., & Kunkel, L. M. (1990). Localization of dystrophin to postsynaptic regions of central nervous system cortical neurons. *Nature*, 348, 725–728. <https://doi.org/10.1038/348725a0>
- Llinás, R., & Sugimori, M. (1980). Electrophysiological properties of in vitro Purkinje cell somata in mammalian cerebellar slices. *The Journal of Physiology*, 305, 171–195. <https://doi.org/10.1113/jphysiol.1980.sp013357>
- Mapelli, J., & D'Angelo, E. (2007). The spatial organization of long-term synaptic plasticity at the input stage of cerebellum. *Journal of Neuroscience: the Official Journal of the Society for Neuroscience*, 27, 1285–1296. <https://doi.org/10.1523/JNEUROSCI.4873-06.2007>
- Maresh, K., Papageorgiou, A., Ridout, D., Harrison, N. A., Mandy, W., Skuse, D., & Muntoni, F. (2023). Startle responses in Duchenne muscular dystrophy: A novel biomarker of brain dystrophin deficiency. *Brain: a Journal of Neurology*, 146, 252–265. <https://doi.org/10.1093/brain/awac048>
- Markati, T., Oskoui, M., Farrar, M. A., Duong, T., Goemans, N., & Servais, L. (2022). Emerging therapies for Duchenne muscular dystrophy. *Lancet Neurology*, 21, 814–829. [https://doi.org/10.1016/S1474-4422\(22\)00125-9](https://doi.org/10.1016/S1474-4422(22)00125-9)
- Márquez-Ruiz, J., & Cheron, G. (2012). Sensory stimulation-dependent plasticity in the cerebellar cortex of alert mice. *PLoS ONE*, 7, e36184. <https://doi.org/10.1371/journal.pone.0036184>
- Mento, G., Tarantino, V., & Bisiacchi, P. S. (2011). The neuropsychological profile of infantile Duchenne muscular dystrophy. *The Clinical Neuropsychologist*, 25, 1359–1377. <https://doi.org/10.1080/13854046.2011.617782>
- Muntoni, F., Mateddu, A., & Serra, G. (1991). Passive avoidance behaviour deficit in the mdx mouse. *Neuromuscular Disorders*, 1, 121–123. [https://doi.org/10.1016/0960-8966\(91\)90059-2](https://doi.org/10.1016/0960-8966(91)90059-2)
- Naidoo, M., & Anthony, K. (2020). Dystrophin Dp71 and the neuropathophysiology of Duchenne muscular dystrophy. *Molecular Neurobiology*, 57, 1748–1767. <https://doi.org/10.1007/s12035-019-01845-w>
- Nicchia, G. P., Rossi, A., Nudel, U., Svelto, M., & Frigeri, A. (2008). Dystrophin-dependent and -independent AQP4 pools are expressed in the mouse brain. *Glia*, 56, 869–876. <https://doi.org/10.1002/glia.20661>
- Nudel, U., Robzyk, K., & Yaffe, D. (1988). Expression of the putative Duchenne muscular dystrophy gene in differentiated myogenic cell cultures and in the brain. *Nature*, 331, 635–638. <https://doi.org/10.1038/331635a0>
- Okamoto, K., Kimura, H., & Sakai, Y. (1983). Effects of taurine and GABA on ca spikes and Na spikes in cerebellar purkinje cells in vitro: Intracellular study. *Brain Research*, 260, 249–259. [https://doi.org/10.1016/0006-8993\(83\)90678-9](https://doi.org/10.1016/0006-8993(83)90678-9)
- Orso, M., Migliore, A., Polistena, B., Russo, E., Gatto, F., Monterubbianesi, M., d'Angela, D., Spandonaro, F., & Pane, M. (2023). Duchenne muscular dystrophy in Italy: A systematic review of epidemiology, quality of life, treatment adherence, and economic impact. *PLoS ONE*, 18, e0287774. <https://doi.org/10.1371/journal.pone.0287774>
- Pascual-Morena, C., Cavero-Redondo, I., Álvarez-Bueno, C., Jiménez-López, E., Saz-Lara, A., Martínez-García, I., & Martínez-Vizcaino, V. (2023). Global prevalence of intellectual developmental disorder in dystrophinopathies: A systematic review and meta-analysis. *Developmental Medicine and Child Neurology*, 65, 734–744. <https://doi.org/10.1111/dmcn.15481>
- Pereira da Silva, J. D., Campos, D. V., Nogueira-Bechara, F. M., Stilhano, R. S., Han, S. W., Sinigaglia-Coimbra, R., Lima-Landman, M. T. R., Lapa, A. J., & Souccar, C. (2018). Altered release and uptake of gamma-aminobutyric acid in the cerebellum of dystrophin-deficient mice. *Neurochemistry International*, 118, 105–114. <https://doi.org/10.1016/j.neuint.2018.06.001>
- Rafael, J. A., Nitta, Y., Peters, J., & Davies, K. E. (2000). Testing of SHIRPA, a mouse phenotypic assessment protocol, on Dmd (mdx) and Dmd (mdx3cv) dystrophin-deficient mice. *Mammalian Genome: Official Journal of the International Mammalian Genome Society*, 11, 725–728. <https://doi.org/10.1007/s003350010149>

- Ramani, P. K., Fawcett, K., Guntrum, D., Samuel, H., Ciafaloni, E., & Veerapandiyan, A. (2023). Epilepsy characteristics in Duchenne and Becker muscular dystrophies. *Child Neurology Open*, *10*, 2329048X231159484. <https://doi.org/10.1177/2329048X231159484>
- Roggeri, L., Rivieccio, B., Rossi, P., & D'Angelo, E. (2008). Tactile stimulation evokes long-term synaptic plasticity in the granular layer of cerebellum. *Journal of Neuroscience: the Official Journal of the Society for Neuroscience*, *28*, 6354–6359. <https://doi.org/10.1523/JNEUROSCI.5709-07.2008>
- Schiffmann, S. N., Cheron, G., Lohof, A., d'Alcantara, P., Meyer, M., Parmentier, M., & Schurmans, S. (1999). Impaired motor coordination and Purkinje cell excitability in mice lacking calretinin. *Proceedings of the National Academy of Sciences of the United States of America*, *96*, 5257–5262. <https://doi.org/10.1073/pnas.96.9.5257>
- Schwaller, B., Meyer, M., & Schiffmann, S. (2002). "New" functions for "old" proteins: The role of the calcium-binding proteins calbindin D-28k, calretinin and parvalbumin, in cerebellar physiology. Studies with knockout mice. *Cerebellum (London, England)*, *1*, 241–258. <https://doi.org/10.1080/147342202320883551>
- Sekiguchi, M., Zushida, K., Yoshida, M., Maekawa, M., Kamichi, S., Yoshida, M., Sahara, Y., Yuasa, S., Takeda, S., & Wada, K. (2009). A deficit of brain dystrophin impairs specific amygdala GABAergic transmission and enhances defensive behaviour in mice. *Brain: a Journal of Neurology*, *132*, 124–135. <https://doi.org/10.1093/brain/awn253>
- Servais, L., Bearzatto, B., Schwaller, B., Dumont, M., De Saedeleer, C., Dan, B., Barski, J. J., Schiffmann, S. N., & Cheron, G. (2005). Mono- and dual-frequency fast cerebellar oscillation in mice lacking parvalbumin and/or calbindin D-28k. *The European Journal of Neuroscience*, *22*, 861–870. <https://doi.org/10.1111/j.1460-9568.2005.04275.x>
- Servais, L., Hourez, R., Bearzatto, B., Gall, D., Schiffmann, S. N., & Cheron, G. (2007). Purkinje cell dysfunction and alteration of long-term synaptic plasticity in fetal alcohol syndrome. *Proceedings of the National Academy of Sciences of the United States of America*, *104*, 9858–9863. <https://doi.org/10.1073/pnas.0607037104>
- Sicot, G., Servais, L., Dinca, D. M., Leroy, A., Prigogine, C., Medja, F., Braz, S. O., Huguet-Lachon, A., Chhuon, C., Nicole, A., Gueriba, N., Oliveira, R., Dan, B., Furling, D., Swanson, M. S., Guerrero, I. C., Cheron, G., Gourdon, G., & Gomes-Pereira, M. (2017). Downregulation of the glial GLT1 glutamate transporter and Purkinje cell dysfunction in a mouse model of myotonic dystrophy. *Cell Reports*, *19*, 2718–2729. <https://doi.org/10.1016/j.celrep.2017.06.006>
- Snow, W. M., Anderson, J. E., & Fry, M. (2014). Regional and genotypic differences in intrinsic electrophysiological properties of cerebellar Purkinje neurons from wild-type and dystrophin-deficient mdx mice. *Neurobiology of Learning and Memory*, *107*, 19–31. <https://doi.org/10.1016/j.nlm.2013.10.017>
- Stay, T. L., Miterko, L. N., Arancillo, M., Lin, T., & Sillitoe, R. V. (2019). In vivo cerebellar circuit function is disrupted in an mdx mouse model of Duchenne muscular dystrophy. *Disease Models & Mechanisms*, *13*, dmm040840.
- Steuber, V., Mittmann, W., Hoebeek, F., Silver, R. A., De Zeeuw, C. Häusser, M., & De Schutter, E. (2007). Cerebellar LTD and pattern recognition by Purkinje cells. *Neuron*, *54*, 121–136. <https://doi.org/10.1016/j.neuron.2007.03.015>
- Sugihara, I., Lang, E. J., & Llinás, R. (1995). Serotonin modulation of inferior olivary oscillations and synchronicity: A multiple-electrode study in the rat cerebellum. *The European Journal of Neuroscience*, *7*, 521–534. <https://doi.org/10.1111/j.1460-9568.1995.tb00657.x>
- Tadayoni, R., Rendon, A., Soria-Jasso, L. E., & Cisneros, B. (2012). Dystrophin Dp71: The smallest but multifunctional product of the Duchenne muscular dystrophy gene. *Molecular Neurobiology*, *45*, 43–60. <https://doi.org/10.1007/s12035-011-8218-9>
- Torriero, S., Oliveri, M., Koch, G., Lo Gerfo, E., Salerno, S., Petrosini, L., & Caltagirone, C. (2007). Cortical networks of procedural learning: Evidence from cerebellar damage. *Neuropsychologia*, *45*, 1208–1214. <https://doi.org/10.1016/j.neuropsychologia.2006.10.007>
- Tuckett, E., Gosetti, T., Hayes, A., Rybalka, E., & Verghese, E. (2015). Increased calcium in neurons in the cerebral cortex and cerebellum is not associated with cell loss in the mdx mouse model of Duchenne muscular dystrophy. *Neuroreport*, *26*, 785–790. <https://doi.org/10.1097/WNR.0000000000000425>
- Uchino, M., Teramoto, H., Naoe, H., Miike, T., Yoshioka, K., & Ando, M. (1994). Dystrophin and dystrophin-related protein in the central nervous system of normal controls and Duchenne muscular dystrophy. *Acta Neuropathologica (Berl)*, *87*, 129–134. <https://doi.org/10.1007/BF00296181>
- Uchino, M., Teramoto, H., Naoe, H., Yoshioka, K., Miike, T., & Ando, M. (1994). Localisation and characterisation of dystrophin in the central nervous system of controls and patients with Duchenne muscular dystrophy. *Journal of Neurology, Neurosurgery, and Psychiatry*, *57*, 426–429. <https://doi.org/10.1136/jnnp.57.4.426>
- Vaillend, C., Billard, J.-M., & Laroche, S. (2004). Impaired long-term spatial and recognition memory and enhanced CA1 hippocampal LTP in the dystrophin-deficient Dmd (mdx) mouse. *Neurobiology of Disease*, *17*, 10–20. <https://doi.org/10.1016/j.nbd.2004.05.004>
- Vaillend, C., Rendon, A., Misslin, R., & Ungerer, A. (1995). Influence of dystrophin-gene mutation on mdx mouse behavior. I. Retention deficits at long delays in spontaneous alternation and bar-pressing tasks. *Behavior Genetics*, *25*, 569–579. <https://doi.org/10.1007/BF02327580>
- van Vreeswijk, C., & Sompolinsky, H. (1996). Chaos in neuronal networks with balanced excitatory and inhibitory activity. *Science*, *274*, 1724–1726. <https://doi.org/10.1126/science.274.5293.1724>
- Vandeputte, C., Taymans, J.-M., Casteels, C., Coun, F., Ni, Y., Van Laere, K., & Baekelandt, V. (2010). Automated quantitative gait analysis in animal models of movement disorders. *BMC Neuroscience*, *11*, 92. <https://doi.org/10.1186/1471-2202-11-92>
- Vicari, S., Piccini, G., Mercuri, E., Battini, R., Chieffo, D., Bulgheroni, S., Pecini, C., Lucibello, S., Lenzi, S., Moriconi, F., Pane, M., D'Amico, A., Astrea, G., Baranello, G., Riva, D., Cioni, G., & Alfieri, P. (2018). Implicit learning deficit in children with Duchenne muscular dystrophy: Evidence for a cerebellar cognitive impairment? *PLoS ONE*, *13*, e0191164. <https://doi.org/10.1371/journal.pone.0191164>
- Waite, A., Tinsley, C. L., Locke, M., & Blake, D. J. (2009). The neurobiology of the dystrophin-associated glycoprotein complex.

- Annals of Medicine*, 41, 344–359. <https://doi.org/10.1080/07853890802668522>
- Wallace, G. Q., & McNally, E. M. (2009). Mechanisms of muscle degeneration, regeneration, and repair in the muscular dystrophies. *Annual Review of Physiology*, 71, 37–57. <https://doi.org/10.1146/annurev.physiol.010908.163216>
- Welsh, J. P., Lang, E. J., Sugihara, I., & Llinás, R. (1995). Dynamic organization of motor control within the olivocerebellar system. *Nature*, 374, 453–457. <https://doi.org/10.1038/374453a0>
- Whitehead, N. P., Yeung, E. W., & Allen, D. G. (2006). Muscle damage in mdx (dystrophic) mice: Role of calcium and reactive oxygen species. *Clinical and Experimental Pharmacology & Physiology*, 33, 657–662. <https://doi.org/10.1111/j.1440-1681.2006.04394.x>
- Wicksell, R. K., Kihlgren, M., Melin, L., & Eeg-Olofsson, O. (2004). Specific cognitive deficits are common in children with Duchenne muscular dystrophy. *Developmental Medicine and Child Neurology*, 46, 154–159. <https://doi.org/10.1111/j.1469-8749.2004.tb00466.x>
- Wu, W.-C., Bradley, S. P., Christie, J. M., & Pugh, J. R. (2022). Mechanisms and consequences of cerebellar Purkinje cell disinhibition in a mouse model of Duchenne muscular dystrophy. *Journal of Neuroscience: the Official Journal of the Society for Neuroscience*, 42, 2103–2115. <https://doi.org/10.1523/JNEUROSCI.1256-21.2022>
- Zanou, N., Schakman, O., Louis, P., Ruegg, U. T., Dietrich, A., Birnbaumer, L., & Gailly, P. (2012). Trpc1 ion channel modulates phosphatidylinositol 3-kinase/Akt pathway during myoblast differentiation and muscle regeneration. *The Journal of Biological Chemistry*, 287, 14524–14534. <https://doi.org/10.1074/jbc.M112.341784>
- Zanou, N., Shapovalov, G., Louis, M., Tajeddine, N., Gallo, C., Van Schoor, M., Anguish, I., Cao, M. L., Schakman, O., Dietrich, A., Lebacqz, J., Ruegg, U., Roulet, E., Birnbaumer, L., & Gailly, P. (2010). Role of TRPC1 channel in skeletal muscle function. *American Journal of Physiology. Cell Physiology*, 298, C149–C162. <https://doi.org/10.1152/ajpcell.00241.2009>
- Zarrouki, F., Goutal, S., Vacca, O., Garcia, L., Tournier, N., Goyenvalle, A., & Vaillend, C. (2022). Abnormal expression of synaptic and Extrasynaptic GABAA receptor subunits in the dystrophin-deficient mdx mouse. *International Journal of Molecular Sciences*, 23, 12617. <https://doi.org/10.3390/ijms232012617>

**How to cite this article:** Prigogine, C., Ruiz, J. M., Cebolla, A. M., Deconinck, N., Servais, L., Gailly, P., Dan, B., & Cheron, G. (2024). Cerebellar dysfunction in the *mdx* mouse model of Duchenne muscular dystrophy: An electrophysiological and behavioural study. *European Journal of Neuroscience*, 60(10), 6470–6489. <https://doi.org/10.1111/ejn.16566>